Functional characterization of virulence factors, thermostable direct hemolysin (Tdh) and calcium response protein D1 (VcrD1) in *Vibrio parahaemolyticus*

Hyeon Jin Noh

Department of Medical Science

The Graduate School, Yonsei University

Functional characterization of virulence factors, thermostable direct hemolysin (Tdh) and calcium response protein D1 (VcrD1) in *Vibrio parahaemolyticus*

Directed by Professor Soon-Jung Park

The Master's Thesis

submitted to the Department of Medical Science,

the Graduate School of Yonsei University

in partial fulfillment of the requirements for the degree of

Master of Medical Science

Hyeon Jin Noh

December 2014

This certifies that the Master's Thesis

of Hyeon Jin Noh is approved.

_____

Thesis Supervisor: Soon-Jung Park

_____

Thesis Committee Member #1: Sang Sun Yoon

_____

Thesis Committee Member #2: Sung Jae Shin

The Graduate School

Yonsei University

December 2014

ACKNOWLEGEMENTS

Apart from my own efforts, my master's thesis would not have been possible without the support of many people. First and foremost, I would like to thank to my supervisor, Prof. Soon-Jung Park, for her continuous guidance, assistance and faith in me. She greatly encouraged me to focus on this study. What I learned from her during last two years will be invaluable experience to me.

I am also grateful to Profs. Sang Sun Yoon and Sung Jae Shin for being thesis committee members for this project and for their passion and encouragement throughout, which have been extremely helpful. They are always available for my questions, and they were positive and offered their time and shared with me their extensive knowledge. And, thanks to Profs. Tai-Soon Yong, Myeong Heon Shin and Hyung-Pyo Kim for giving me informative advice and for showing genuine interest.

Epecially, I would like to show my appreciation to Prof. Kyu-Ho Lee. I can't say enough to thank him for his advice and help. His guidance inspired me to pursue my dreams in science and gave me an opportunity to realize it.

I wish to express my sincere gratitude to my fellow labmates, Juri Kim, who supports me with her abundant knowledge, and

Mee Young Shin, who helps me with the more technical experiments. I also deeply thank Hye-Yeon Lee, Min Jung Kim and Sara Nagami. I am pleased and blessed to work with such good people during my master's project.

Last but not least, I wish to express my love and gratitude to family. I am forever indebted to my parents and brother. They gave me moral and spiritual support and show me unconditional and endless love every day.

Hyeon Jin Noh

TABLE OF CONTENTS

LIST OF FIGURES

LIST OF TABLES

ABSTRACT

Functional characterization of virulence factors, thermostable direct hemolysin (Tdh) and calcium response protein D1 (VcrD1) in *Vibrio parahaemolyticus*

Hyeon Jin Noh

Department of Medical Science

The Graduate School, Yonsei University

(Directed by Professor Soon-Jung Park)

Vibrio parahaemolyticus, a gram-negative marine bacterium, is a worldwide cause of foodborne gastroenteritis. Thermostable direct hemolysin (Tdh) is a factor responsible for the Kanagawa phenomenon caused by pathogenic *V. parahaemolyticus*.

In chapter I, expression of Tdh was examined under various culture conditions. Two *tdh* genes, *tdhA* and *tdhS*, were identified in the genomic sequence of wild-type

V. parahaemolyticus. Reporter fusions between these *tdh* promotors and the luciferase gene indicated that the *tdhA* gene is expressed higher than *tdhS* under the conditions tested, and expression of both *tdh* genes was induced by the presence of an iron chelator or crude bile in the medium. Candidate transcription factor(s) for bile-mediated *tdh* expression were isolated by ligand fishing experiments. Through Western blot analysis and fusion assay on *ΔtoxR* mutant *V. parahaemolyticus,* a global regulator, ToxR (cholera toxin transcriptional activator) was found to control bile-induced expression of the *tdhA* gene. Direct binding of ToxR protein to the *tdhA* promoter was shown by gel-shift assays. In addition, the cytotoxic role of TdhA was observed by treating human gastrointestinal HT-29 cells with recombinant TdhA (rTdhA). HT-29 cells treated with rTdhA demonstrated considerable morphological changes under transmission electron microscopy. Both apoptotic and necrotic cell deaths were detected by staining with Annexin V and PI, respectively. Cytotoxicity of rTdhA was reduced by the RIP-1-mediated necroptosis inhibitor, necrostatin-1, indicating that rTdhA causes host cell death by necroptosis. These data clearly showed that expression of Tdh is modulated by certain physiological signals, such as iron depletion and presence of bile, and this toxin is quite capable of killing host cells mainly via necrosis.

In chapter II, VcrD1 protein is highlighted as a component of type III secretion system (T3SS) 1 in *Vibrio parahaemolyticus*. A comparative analysis of secretomes of wild-type and *ΔvcrD1* strains revealed that the mutant was defective in secretion of at least 19 proteins including several flagellar components. Western blot analyses

using specific antibodies confirmed that the secretion of at least four flagellar components, such as FlaA, FlgL, FlgE, and FlgM, was affected by the *vcrD1* mutation, which was consistent with decreased motility on soft agar plates and the non-flagellated morphology of the mutant. The *ΔexsA* variant, another T3SS mutant, did not showed reduced motility, but exhibited a non-motile phenotype with the *ΔvcrD1* mutation. Complementation of wild-type *vcrD1* gene into the *ΔvcrD1* mutant resulted in restored motility. Fractionation of bacterial cytoplasm from the periplasm and membrane revealed lower levels of FlaA and FlgM in the cytoplasm, indicating that VcrD1 might regulate the expression of flagellar genes in addition to the secretion of flagellar components in *V. parahaemolyticus*. Quantitative RT-PCR assays of seven representative flagellar genes in the wild-type and Δ*vcrD1* mutant strains demonstrated that transcript levels of two early flagellar genes, *flaK* and *flaL,* were not affected by *vcrD1* mutation, whereas the middle and late flagellar genes were down-regulated by the *vcrD1* mutant. This study raises the possibility that VcrD1 plays a role in flagellar morphogenesis in *V. parahaemolyticus* by regulating the expression and secretion of flagellar components.

Key words: *vibrio parahaemolyticus*, thermostable direct hemolysin, *vcrD1*

Chapter I

Expression patterns and cytotoxic role of

V. parahaemolyticus Tdh

I. INTRODUCTION

Vibrio parahaemolyticus is a common inhabitant of marine and estuarine environments including water, sediment, suspended particles, planktons, and shellfishes[1]. An outbreak of seafood infection caused by *V. parahaemolyticus* had been reported in Japan in 1950 for the first time[2]. Gastrointestinal infections due to *V. parahaemolyticus* demonstrated diverse clinical symptoms including mild diarrhea with a duration of 2-3 days, abdominal cramps, nausea, vomiting, headache, low-grade fever, and chills[3]. This microorganism possesses a variety of virulence determinants, such as an adhesin, toxins, and secreted effectors involved in attachment, cytotoxicity, and enterotoxicity[4]. Bacterial ability to lyse red blood cells on Wagatsuma's agar had been defined as an indicator for pathogenic *V. parahaemolyticus* and referred to as the Kanagawa phenomenon (KP)[5]. A correlation between the KP^+ phenotype of *V. parahaemolyticus* and its virulence in humans has been confirmed by Sakazaki et al. based on their observation that only KP^+ strains proliferate selectively in the human intestine[6].

Well-known virulence factors of *V. parahaemolyticus* are the type III secretion systems. Interestingly, genome sequencing of clinical strains of *V. parahaemolyticus* revealed that the strains possess two sets of type III secretion system (TTSS1 and TTSS2). The TTSSs encode a molecular syringe-like apparatus frequently used by diverse Gram-negative bacteria when they deliver their virulence factors into the cytosol of eukaryotic cells[7]. The microbial proteins injected into the

host cell are called effectors. Upon translocation of these effectors into the target host cell, these molecules modulate a wide variety of cellular functions of the host cells, which include phagocytosis, host defense, and apoptosis. Investigation of the TTSSs of *V. parahaemolyticus* demonstrated that TTSS1 is responsible for cytotoxicity to HeLa cells, whereas TTSS2 plays a role in enterotoxicity in a rabbit model[8].

The thermostable direct hemolysin (Tdh) is another virulence factor of *V. parahaemolyticus*. Especially, KP^+ *V. parahaemolyticus* strains were found to have two copies of *tdh* genes (*tdhA* and *tdhS*)[9]. In the KP^+ strain, the expression level of the *tdhA* gene was higher than that of the *tdhS* gene[10]. Both genes show a 97% sequence identity between each other[11]. Purified thermostable direct hemolysin was found to be responsible for the KP phenotype of *V. parahaemolyticus,* which causes fluid accumulation in the ligated mouse ileum, and for cytotoxicity against cultured mammalian cells[12,13]. This protein is unique in its stability to withstand heating at 100°C for 10 min and its activation by Ca^{2+}[14,15]. Biochemical characterization of Tdh demonstrated that it functions as a pore-forming toxin as a homotetramer and each subunit has 165 amino acid residues. This toxin exhibited ion channel-like activity in lipid bilayers with relatively low ion selectivity[16]. It had been reported that Tdh displays several biological attributes including enterotoxicity, cytotoxicity, cardiotoxicity, and hemolytic activity[17,18,19,20].

Despite extensive investigation of Tdh, little information is available with respect to the regulation mechanism of how Tdh toxin is made under diverse

environmental conditions. In this study, transcription of two *tdh* genes, *tdhA* and *tdhS*, was monitored under various stressed conditions.

Survival of bacterial species under diverse stressed conditions is a critical step for pathogenic bacteria to maintain their pathogenicity[21]. Expression of virulence factors is regulated in a coordinated manner by common global regulators in response to environmental conditions, and this coordinated regulation is crucial to the overall success of the pathogens during infection[22,23].

One of the environmental factors was oxidative stresses that pathogens may encounter during infection of the host cells. The host innate immune system generates reactive oxygen species and nitric oxide as bacteriocidal agents, and both require O_2 for their production. Therefore, the ability to adapt to changes in O_2 availability is crucial for many bacterial pathogens, as many niches within a host are hypoxic. Pathogenic bacteria have evolved transcriptional regulatory systems that detect these gases and respond by reprogramming gene expression. Bacterial genetic responses to oxidative stress are controlled by two major transcriptional regulators: OxyR and SoxRS. *Escherichia coli* has a specific defense mechanism against peroxides, mediated by the transcriptional activator OxyR, and another defense mechanism against superoxide, controlled by the SoxRS system[24].

The second factor tested was iron availability. Iron is an essential element for living organisms required for many biological activities including oxygen transport, photosynthesis, the trichloroacetic acid cycle, and respiration[25]. Availability of a soluble form of iron is critical for virulence of pathogenic microbes because

solubility of iron is extremely low at neutral pH. On the other hand, an excess of intracellular iron is harmful to cells because it leads to the production of toxic free radicals[26]. In pathogens, expression of virulence-associated genes was modulated by iron concentration[27,28,29]. Ferric uptake regulator (Fur) is the regulator responsible for iron control of expression of virulence genes. Fur is a small protein that regulates expression of multiple gene by binding to an upstream sequence called the Fur box, which binds with iron[30,31]. The Fur protein of *V. vulnificus* functions as a homodimer of approximately 16-kDa monomers and affects the expression of diverse genes, including those for iron utilization and superoxide dismutase[32]. The iron-sulfur cluster regulator (IscR) is another regulator involved in iron control. IscR containing the Fe-S cluster as a cofactor carries out multiple important cellular processes such as electron transfer, metabolic reactions, and gene regulation[33,34]. IscR functions as a sensor of cellular Fe-S cluster status and regulates Fe-S cluster biogenesis homeostatically[35]. IscR expression was found to be induced by exposure of the pathogen to host cells[36].

The third environmental factor was bile, which was included to examine its effect on expression of Tdh in *V. parahaemolyticus*. In the intestine, pathogenic bacteria may encounter concentrations of bile with a strong detergent-like property. Noh and Gilliland have reported that the presence of oxgall in reaction buffer increased the cellular permeability of *Lactobacillus acidophilus*, thereby enhancing its enzymatic activity[37]. Osawa reported that conjugated bile acids enhance Tdh production by *V. parahaemolyticus,* suggesting that the bile acids play a key role in

the pathogenicity of *V. parahaemolyticus* during its natural infection of the human intestine. However, the mechanism underlying the effect of bile on synthesis of Tdh has not been characterized. Numerous effects of crude bile on *V. cholerae* have been described. In the classical biotype *V. cholerae*, crude ox bile extract decreased expression of the virulence factors such as cholera toxin (CT) and toxin-coregulated pilus (TcpA). A transcriptional regulator responsible for CT production is ToxR, a 32-kDa inner-membrane protein[38], which binds to the upstream region of the *toxT* gene, encoding another transcriptional activator of virulence factors of *V. cholerae*[39]. The effect of bile on CT production was found to be dependent on ToxR by possibly altering expression of outermembrane protein[40,41,42].

In addition to study of the expression of Tdh under diverse environmental conditions, Tdh toxin was prepared from *V. parahaemolyticus* and its action against the host cells was examined.

II. MATERIALS AND METHODS

1. Cultures for bacteria and human cells

Bacterial strains and plasmids used in this study are listed in Table 1. *Escherichia coli* strains used for plasmid preparation and the conjugational transfer of plasmid were grown in Luria-Bertani (LB: 1.0% bacto-tryptone, 0.5% yeast extract, 1.0% NaCl) broth or on LB plates containing 2% (wt/vol) agar. *Vibrio parahaemolyticus* RIMD2210633 (ATCCBAA-238; American Type Culture Collection, Mannassas, VA) was cultured in LBS medium supplemented with 3% (wt/vol) sodium chloride, unless stated otherwise. *V. parahaemolytics* and *E.coli* strains were cultivated at 37°C. Antibiotics were used at the following concentrations: ampicillin 100 μg/ml, kanamycin 100 μg/ml, chloramphenicol 25 μg/ml, and tetracycline 15 μg/ml for *E. coli*; ampicillin 500 μg/ml, kanamycin 300 μg/ml, chloramphenicol 2 μg/ml, and tetracycline 3 μg/ml for *V. parahaemolyticus*. All medium components were purchased from Difco (Lawrence, KS), and the chemicals and antibiotics were sourced from Sigma (St. Louis, MO).

A human colorectal carcinoma cell line HT-29 (HTB-38; American Type Culture Collection) was cultured in Dulbecco's modified Eagle's medium (DMEM; Gibco BRL, Karlsruhe, Germany) supplemented with 10% FBS and 100 U/ml penicillin G. Samples were incubated at 37°C in a humid atmosphere of 5% CO_2.

2. Luminescence assays under environmental conditions

Plasmids, pLUXtdhA, and pLUXtdhS[43] were used for luminescence assays to monitor expression levels of *tdhA* and *tdhS* genes, respectively. The promoter regions of *tdhA* or *tdhS* genes were cloned into pHK0011 containing promoterless *luxAB* genes[44], and the resultant plasmids were mobilized into *V. parahaemolyticus* by conjugation.

The effect of iron availability on the expression of *tdh-luxAB* was examined by adding 200 μM 2,2'-dipyridyl or 20 μM ethylenediamine-*N*,*N*′-diacetic acid (EDDA) to bacterial culture at the early exponential stage (OD_{595}= 0.6). Expression of *tdh-luxAB* was also examined under oxidative stresses by including 0.1 mM hydrogen peroxide or 0.1 mM paraquat to cultures at the early exponential stage (OD_{595}= 0.6). *V. parahaemolyticus* carrying the *tdh-luxAB* fusion plasmid was grown in the presence of 0.05% (wt/vol) crude bile or 0.005% (wt/vol) bile salt and monitored for luciferase activity. The light produced by exconjugant *V. parahaemolyticus* harboring the transcription reporter fusion plasmid was measured in the presence of 0.006% (vol/vol) *n*-decyl aldehyde using a luminometer (TD-20/20 Luminometer, Turners Designs). Specific bioluminescence was calculated by normalizing the relative light units (RLU) with respect to cell mass (OD_{595}).

3. Construction of deletion mutants of *V. parahaemolyticus*

A. *Δfur* mutant

Primers used in this study are listed in Table 2. An 800-bp PCR product containing the *fur* upstream region was amplified using primers, fur-upF and fur-upR, and then cloned into pBluescriptSKII (+) to produce pSKfur01. A 656-bp PCR product containing the downstream region of the *fur* gene was made using fur-downF and fur-downR, and then cloned into the corresponding sites of pSKfur01, resulting in pSKfur02. The *nptI* gene encoding a kanamycin-resistant enzyme was isolated from pUC4K (Amersham), and inserted into pSKfur02 to generate pSKfur03. The *Apa*I–*Sac*I DNA fragment of pSKfur03 was ligated into pDM4[45] to produce pDM4-Δfur. The resultant plasmid in the *E. coli* SM10λ*pir* strain was mobilized to *V. parahaemolyticus* RIMD2210633, and the exconjugants were selected. A colony with characteristics indicating a double homologous recombination event was isolated as described[46]. Deletion of the *fur* gene in mutant candidates was confirmed by PCR with primers, fur-upF and fur-downR.

B. *ΔiscR* mutant

A *ΔiscR* strain was constructed via a similar procedure described for the *fur* mutant. An 858-bp upstream and a 915-bp downstream region of *iscR* gene were produced using primer sets of iscR-upF /iscR-upR and iscR-downF /iscR-downR, respectively. These PCR products were used to make pSKiscR02, which contains

upstream and downstream regions of the *icsR* gene. A 1.7-kb *Apa*I-*Sac*I DNA fragment of pSKiscR02 was cloned into pDM4 to generate pDM4-ΔicsR. The resultant plasmid was used to make *ΔiscR V. parahaemolyticus*. Candidate mutant colonies were examined for their *iscR* loci by PCR with primers, iscR-upF and iscR-downR.

C. *Δ toxR* mutant

A plasmid (pSKtoxR03) including the upstream (820-bp) and the *nptI* gene encoding a kanamycin-resistant enzyme and downstream (551-bp) regions of the *toxR* gene, which have been amplified by the following primer sets, toxR-upF /toxR-upR and toxR-downF/toxR-downR, respectively. The *Apa*I-*Sac*I DNA fragment of the resultant plasmid was ligated into pDM4 to produce pDM4-ΔtoxR, which was used to make the *ΔtoxR* mutant, as described above.

4. Ligand fishing experiments

The DNA fragment used as bait was amplified with primers, tdhA-F1 and tdhA-R1, which contained the 468-bp promoter region of the *tdhA* gene. As a control DNA, the 500-bp coding region of TdhA was made with two primers, tdhA-F2 and tdhA-R2. One hundred micrograms of each DNA was loaded on to a NeutrAvidin column as directed by the manufacturer (Pierce, Illinois, USA).

Wild-type *V. parahaemolyticus* was grown up to OD_{595}= 2 in LBS broth in the

presence or absence of 0.05% (wt/vol) crude bile. The harvested cells were resuspended in the binding buffer (40 mM HEPES-KOH, pH 7.9, 100 mM KCl, 10 mM $MgCl_2$, 2 mM DTT, and 10% glycerol), and then lysed by sonication. Soluble proteins were prepared by centrifugation at 3000 rpm for 20 min, and 50 mg of supernatant protein was loaded on to the column immobilized either with the *tdhA* promoter or control DNA fragment. After two washes with 5 ml of binding buffer, the bound proteins were eluted with 1 ml of 0.1% SDS. The eluted proteins were concentrated by freeze-drying, and then resuspended in 100 μl of deionized water. Ten micrograms of the protein sample was analyzed by SDS-PAGE. Protein bands appearing only in the column coupled to *tdhA* promoter DNA were excised, and treated by in-gel digestion with trypsin (Saint Louis, Missouri, USA). Digested products were analyzed by quadrupole TOF (Q-TOF) in addition to MALDI-TOF MS. Product ion spectra were collected in the information-dependent acquisition (IDA) mode and were analyzed with an Agilent 6530 accurate-mass Q-TOF MS. For the Q-TOF liquid chromatography-tandem MS (LC-MS/MS) data sets, tandem mass spectra were submitted to our MASCOT in-house database search engine (Vibrio DB). Mass tolerances of 100 ppm and 0.2 Da were used for precursor and fragment ions, respectively. For protein identification, a MASCOT ion score of 45 was used as the criterion.

5. Preparation of secreted proteins from *V. parahaemolyticus*

The wild-type or *toxR* mutant of *V. parahaemolyticus* was grown in LBS broth. At OD_{595} 0.6, each sample of cultured cells was divided into two aliquots, and to one of the two 0.05% crude bile was added. Total secreted protein from *V. parahaemolyticus* was extracted by culture supernatant at OD_{595} 2. Bacterial cells were removed by filtering using 0.2 μm – pore size membrane filter (Millipore, Massachusetts, USA). Secretome was concentrated using centricon YM-10 (Millipore, Darmstadt, Germany).

6. Western blot analysis

Secreted protein was separated by SDS-PAGE, and transferred on to a polyvinyl idenefluoride (PVDF) membrane (Millipore). The membrane was incubated with polyclonal rat anti-TdhA antibodies (1:5000) or anti-OmpU antibodies (1:5000) in a blocking solution tris-buffered saline with Tween 20 (TBST; 50 mM Tris-HCl, 5% skim milk, and 0.05% Tween 20) at 4°C overnight. Following incubation with horseradish peroxidase (HRP)-conjugated secondary antibodies, the immunoreactive protein was visualized using an enhanced chemiluminescence (ECL) system (Amersham Phamacia). Membranes were incubated in a stripping buffer (Thermo Scientific, Rockford, IL, USA) at room temperature for 30 min, and then reacted with polyclonal rat antibodies specific to the FlaA of *V. parahaemolyticus.*

The membrane incubated with polyclonal mouse anti-His antibodies (1:5000) was

incubated with alkaline phosphatase (AP)-conjugated rat anti-mouse IgG (Sigma) (1:3000). Immunoreactive protein was visualized using the nitro-blue tetrazolium (NBT) / 5-bromo-4-chloro-3-indolyl phosphate (BCIP) system (Promega).

7. Expression and purification of recombinant ToxR

A 516-bp DNA fragment encoding the cytoplasmic portion of ToxR (from amino acid 1 to 172) was amplified by PCR using the primers ToxR-F and ToxR-R, and then cloned into the pET21b (+) vector (Novagen, Darmstadt, Germany) to generate pETToxR. The resultant plasmid was transformed into *E. coli* BL21 (DE3), and the expression of the recombinant cytoplasmic ToxR (rcToxR) was induced with 1 mM Isopropyl β-D-1-thiogalactopyranoside (IPTG) as a histidine-tagged form. Harvested bacterial cells were resuspended in a lysis buffer (50 mM sodium phosphate, 300mM NaCl) and lysed by sonication. Soluble fraction was collected by centrifugation at 7,000 rpm for 10 min, and passed through a Talon affinity column according to the manufacturer's directions (Clontech, CA, USA).

8. Electrophoretic mobility shift assay

The 235-bp DNA containing the *tdhA* promoter region (from -220 to +15) was synthesized with primers, tdhA-EMSAF and tdhA-EMSAR. This DNA fragment was labeled with [γ-^{32}P] ATP using T4 polynucleotide kinase. A labeled DNA probe (500 nM) was incubated at various concentrations of rcToxR (50 - 200 nM) for 30 min at 37^{o}C in a reaction buffer (10 mM Tris-borate, pH 8.0, 100 μg/ml bovine

serum albumin, 10% (vol/vol) glycerol, 40 mM KCl, 1 mM $MgCl_2$, 100 μM $MnCl_2$ and 5 μg/ml single-strand DNA). After reactions were stopped, aliquots of the reaction mixtures were separated on 6% non-denaturing polyacrylamide gel. For competition analysis, 1μM unlabeled DNA probe was included in the reaction mixture. Gels were exposed to a BAS-MP 2040s imaging plate (Fujifilm, Tokyo, Japan), and scanned by using a BAS-1500 instrument (Fujifilm, Tokyo, Japan). The intensities of the bands were measured using the Multi Gauge software program, version 3.0 (Fujifilm, Tokyo, Japan).

9. Purification of TdhA from *V. parahaemolyticus*

The signal peptide of the putative amino acid sequence of TdhA was examined using the SignalP 4.1 server (http://www.cbs.dtu.dk/services/SignalP/). The SignalP produces three output scores for each position in the input sequence: C-score (raw cleavage site score), S-score (signal peptide score), Y-score (combined cleavage site score). A combination of the C-score and the slope of the S-score results in cleavage site prediction. A DNA fragment including the *tdhA* promoter region and open reading frame (ORF) of TdhA (from -529 to +567 with respect to +1, initiation codon of TdhA) was amplified by PCR using the primers tdhA-F3 and tdhA-R3. The resultant PCR product was cloned into the pRK415 vector[47], from which TdhA can be expressed as a secreted form tagged with five histidines at its C terminus. The resultant plasmid, pRKtdhA, was transformed into an *E. coli* SM10λ*pir* strain to conjugate with *V. parahaemolyticus* RIMD2210633. To collect the secreted

rTdhA, conjugated *V. parahaemolyticus* was cultivated in LBS broth at 37°C with shaking. Expression of the His-tagged rTdhA was induced with 0.05% (wt/vol) crude bile (Sigma) at OD_{595} 0.6. Three hours after adding crude bile, the cells were centrifuged at 8000 rpm for 15 min at 4°C. Supernatants obtained after centrifugation were passed through a 0.2 μm – pore size membrane filter (Corning, NY, USA). Proteins were concentrated using Centricon YM-10 (Millipore, Darmstadt, Germany) at 4°C. To purify rTdhA, Talon affinity chromatography was used according to the manufacturer's directions (Clontech, CA, USA).

10. Morphologic observation of HT-29 cells via transmission electron microscopy (TEM)

HT-29 cells were seeded in a 24-well plate (2×10^5 cells per well) and incubated at 37 °C for 24 hr. At 70% confluence, prepared cells were treated with 0.5 μM or 2 μM rTdhA at 37°C for 3 hr. After washes with pre-cooled phosphate-buffered saline (PBS: 137 mM NaCl, 2.7 mM KCl, 10 mM Na_2HPO, and 2 mM KH_2PO, pH 7.4), the cells were fixed with 2% glutaraldehyde/2% paraformaldehyde solution at 4°C, and then embedded in paraffin. The sections of the prepared cells were observed under TEM (Philps/FEI Co., Oregon, USA), and the acquired images were captured using a MegaView 3 camera (Olympus Soft Imaging Solutions, Münster, Germany).

11. Annexin Ⅴ and PI staining and confocal microscopy

HT-29 cells were seeded in a 6-well plate (8×10^5 cells per well), and incubated at 37°C for 24 hr. Prior to treatment with rTdhA, HT-29 cells were starved for 1 hr in serum-free DMEM. After washing with FBS-free medium, the cells were treated with 1.5 μM rTdhA at 37°C for 3 hr. As a control, the cells were incubated with 0.2% DMSO for 3 hr, whereas another set of cells was treated with 2 μM staurosporin for 3 hr as a positive control for apoptotic cell death. The cells were then stained with Annexin Ⅴ and/or propidium iodide (PI) using the GFP–Certified™ Apoptosis/Necrosis Detection Kit (Enzo Life Sciences, NY, USA) according to the manufacturer's instruments. The slides were then reacted with 4',6-diamidino-2–phenylindole (DAPI; Sigma), rinsed with PBS, and mounted with anti-fade mounting medium (Vectashilde; Vector, Burlingame, CA). They were then observed with a Zeiss LSM 510 laser scanning confocal microscope (Zeiss, Oberkochen, Germany). The images were collected with serial sections at 0.5-μm intervals, and analyzed with Zeiss LSM image browser software (Zeiss).

12. Flow cytometric measurement of the cell death

HT-29 cells were seeded in a 12-well plate (5×10^5 cells per well), and incubated at 37°C for 24 hr. After 1 hr starvation in serum-free DMEM, the cells were treated with 2 μM rTdhA at 37°C for various periods (30 min to 6 hr). As a positive control for cell death, another set of cells was treated with 10 mM hydrogen peroxide for 3 hr. Cells were then stained with Annexin V (BD Pharminogen, New

Jersey, USA) or PI at a final concentration of 0.5 μg/ml, and the degrees of dye-binding were assessed using fluorescence-activated cell sorting (FACS) analysis. FACS analyses were performed on at least 10,000 cells per sample with a FACScan (Becton Dickinson, New Jersey, USA).

13. Cytotoxicity assay

HT-29 cells seeded in a 96-well plate (3×10^4 cells per well) were treated with various concentrations of rTdhA (from 0.5 μM to 1.5 μM) for 3 hr. The release of lactate dehydrogenase (LDH) into the medium was assayed by using the Cytotox96 nonradioactive cytotoxicity kit (Promega, Wisconsin, USA) according to the manufacturer's instruction. Three hours following treatment of rTdhA, the supernatants were collected and assayed for LDH activities. The LDH release was calculated according to the following equation: [(OD_{490} of experimental release - OD_{490} of spontaneous release)/(OD_{490} of maximum release - OD_{490} of spontaneous release)] x 100. The spontaneous release is the amount of LDH released from the cytoplasm of untreated HT-29 cells, whereas the maximum release is the amount of LDH released by complete lysis of untreated HT-29 cells.

14. Pretreated HT-29 cells with inhibitor

To investigate the role of signaling components in TdhA-induced cell death, HT-29 cells were treated with selective inhibitor prior to incubation with rTdhA, and their viabilities were compared with those of untreated cells using LDH assays as

described above.

15. Statistical analysis

Data are presented as the means ± standard deviation from three independent experiments. Statistical analyses were performed using the student's t test (SYSTAT, SigmaPlot version 11; Systat Software Inc. Chicago, IL) to evaluate the statistical significance of the results. Differences were considered significant when $P < 0.05$. Data with $P < 0.01$ are indicated with two asterisks(**), whereas data with P-values between 0.01 and 0.05 are indicated with a single asterisk(*).

Table1. Bacterial strains and plasmids used in this study

Strains /plasmid	Description	Source / reference
E. coli		
DH5α	*supE44, ΔlacU169* (Φ80 *lacZ* ΔM15), *hsdR17, recA1, endA1, gyrA96, thi-1, relA1*	Invitrogen
SM10λ*pir*	*thi thr leu tonA lacY supE recA*::RP4-2-Tc::Mu λ*pir*, OriT of RP4, Km^r, conjugational donor	48
BL21(DE3)	*E. coli* B F- *dcm ompT hsdS* (r_B-m_B-) *gal λ* (DE3)	Invitrogen
Vibrio parahaemolyticus		
RIMD2210633	KP positive, serotype O3:K6	ATCC
Δfur	*fur* deletion mutant derived from RIMD2210633	This study
ΔiscR	*iscR* deletion mutant derived from RIMD2210633	This study
ΔtoxR	*toxR* deletion mutant derived from RIMD2210633	This study
V. para_tdhA	RIMD2210633 conjugated with the pRK415 plasmid expressing *tdhA*	This study
Plasmids		
pHK0011	pRK415 with promoterless *luxAB*;Tc^r	44
pLuxtdhA	pHK0011, *tdhA –luxAB* transcriptional fusion	43
pLuxtdhS	pHK0011, *tdhS –luxAB* transcriptional fusion	43
pBluescript SK II(+)	Cloning vecter; *ori*, *oriF1*, *lacZ*; Ap^r	Stratagene

pSKfur01	pBluescript SK II(+), 800-bp upstream region of *fur*	This study
pSKfur02	pSKfur01,656-bp downstream region of *fur*	This study
pSKfur03	pSKfur02 containing *netI* gene	This study
pUCK4	pUC4 with *nptI*, Ap^r; Km^r	Pharmacia Biotech
pDM4	Suiside vector; oriR6K; Cm^r	45
pDM4-Δfur	pDM4 contaning *A*paI and *S*acI fragment of *fur*	This study
pSKiscR01	pBluescript SK II(+), 858 bp upstream region of *iscR*	This study
pSKiscR02	pSKiscR01, 1773-bp downstream region of *iscR*	This study
pDM4-ΔiscR	pDM4 contaning *A*paI and *S*acI fragment of *iscR*	This study
pSKtoxR01	pBluescript SK II(+), 820 bp upstream region of *toxR*	This study
pSKtoxR02	PSKtoxR01, 1371-bp downstream region of *toxR*	This study
pSKtoxR03	pSKtoxR02 containing *netI* gene	This study
pDM4-ΔtoxR	pDM4 contaning *A*paI and *S*acI fragment of *toxR*	This study
pET21b	Expression vector, Ap^r	Novagen
pET-toxR	pET21b containing 516-bp N-terminus of *toxR*	This study
pRK415	Broad-host-range plasmid; Tc^r	47
pRK-tdhA	pRK415 containing *tdhA* covering from -529 to +567	This study

∗Ap^r, ampicillin resistance; Km^r, kanamycin resistance; Cm^r, chloramphenicol resistance; Tc^r, tetracycline resistance

Table2. Primers used in this study

Primer name	Nucleotide sequence (5'-3')	Enzyme site
Construction of mutant strains		
fur-upF	ATGCGGGCCCTTAAGCAGATTTACGAAGA	*A*paI
fur-upR	ATGCGGATCCATACTTTCCCGTTGGATCATC	*B*amHI
fur-downF	ATGCGGATCCTTTGCTTATAGATTAAAAATA	*B*amHI
fur-downR	ATGCGAGCTCCGTTTACTCGTGAAGTTTGGA	*S*acI
iscR-upF	ATGCGGGCCCGTAGCAATCATAGATGTTGG	*A*paI
iscR-upR	ATGCCTGCAGACCACACCGTAT CCACATGGTTT	*P*stI
iscR-downF	ATGCCTGCAGCGGTCAGCATTTTACATTGGA	*P*stI
iscR-downR	ATGCGAGCTCCGCTGCTCTAGGTCACCGTT	*S*acI
toxR-upF	ATGCGGGCCCGAAGAATAATGTCGGTACCAC	*A*paI
toxR-upR	ATGCCTGCAGTTAGTTCTTCTTAGATGGATG	*P*stI
toxR-downF	ATGCCTGCAGAGGAGGCCAGCATGAAGATT	*P*stI
toxR-downR	ATGCGAGCTCTTGCCCCCTTATCACTAAT	*S*acI
For ligand fishing		
tdhA-F1	biotin-AGATAGAACTTACCTCCCTAAAAGCAAT CATTA	
tdhA-R1	AAAAAAACCTCTGAATTGATTAATAACTTTGCC	
tdhA-F2	biotin-ATGAAGTACCGATATTTTGCA	
tdhA-R2	CCACTCTCATATGCTTCTACA	

For recombinant proteins

ToxR-F	GAATTCGATGACTAACATCGGCACCAAA	*E*coRI
ToxR-R	CTCGAGAGAAGCCACAGGTGCTTTTTC	*X*hoI
tdhA-F3	ATGCAAGCTTCTGTGTTTAAAATATTAATTG	*H*indIII
tdhA-R3	ATGCGGATCCTTAGTGGTGGTGGTGGTG GTGTTGTTGATGTTTACATTCAAA	*B*amHI

For gel shift assay

tdhA-EMSAF	TACCAAGCGATAAGGCATTAA
tdhA-EMSAR	AATATCGGTACTTCATAAAAA

*Restriction enzyme sites are underlined; biotin, 5'-biotinylation

III. RESULTS

1. Effect of oxidative stresses on the level of *tdh* expressions

To examine whether various environmental conditions modulate expression of two *tdh* genes, *tdhA* and *tdhS*, transcription reporter fusions between the promoter region of *tdhA* or *tdhS* gene and *luxAB* genes were constructed, and their transcriptional levels were monitored by measuring luciferase activity in wild-type *V. parahaemolyticus*.

The role of reactive oxygen species (ROS) in *tdhA* and *tdhS* expression was observed by adding 0.1 mM hydrogen peroxide (Fig. 1A and 1C, respectively) or 0.1 mM paraquat (Fig. 1B and 1D, respectively) into the cultures of *V. parahaemolyticus*. Under normal conditions, luciferase activity of p*tdhA*::*luxAB* was dramatically higher (~60,000 RLU/OD_{595}) than p*tdhS*::*luxAB* (~6,000 RLU/OD_{595}), while growth of *V. parahaemolyticus* was not significantly affected by the presence of hydrogen peroxide (Fig. 1A and 1C) or paraquat (Fig. 1B and 1D). Addition of hydrogen peroxide or paraquat did not result in significant alteration in luciferase activity of *tdhA::luxAB* fusion. In the same manner, activity of the *tdhS::luxAB* fusion was not affected by hydrogen peroxide (Fig. 1C) or paraquat (Fig. 1D). These results indicate that transcription of both *tdhA* and *tdhS* genes is not regulated by oxidative stresses.

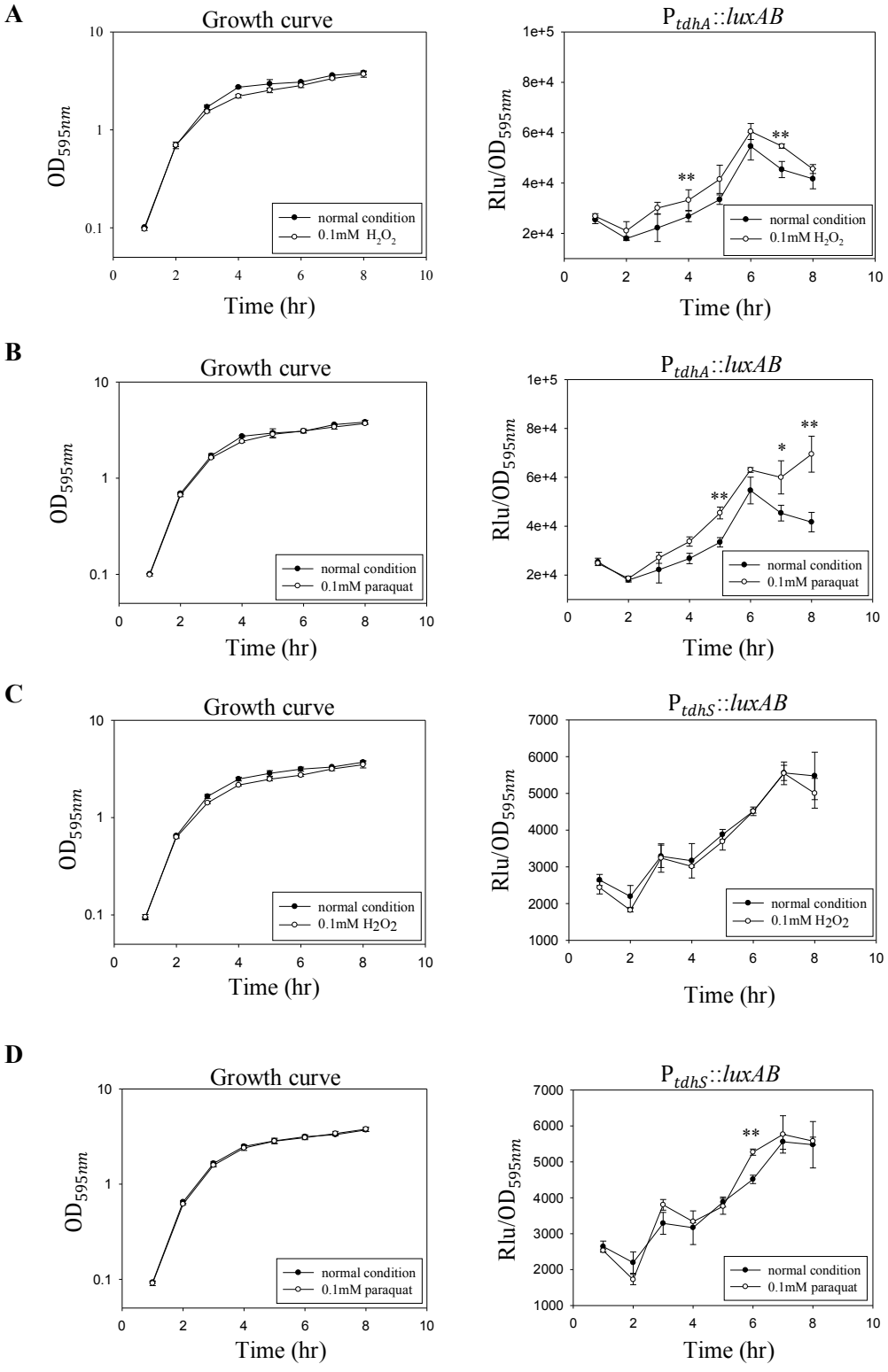
A
Growth curve
OD_{595nm}
Time (hr)
normal condition
0.1mM H_2O_2
P_{tdhA}::*luxAB*
Rlu/OD_{595nm}
**
**
B
Growth curve
OD_{595nm}
Time (hr)
normal condition
0.1mM paraquat
P_{tdhA}::*luxAB*
Rlu/OD_{595nm}
**
*
**
C
Growth curve
OD_{595nm}
Time (hr)
normal condition
0.1mM H_2O_2
P_{tdhS}::*luxAB*
Rlu/OD_{595nm}
D
Growth curve
OD_{595nm}
Time (hr)
normal condition
0.1mM paraquat
P_{tdhS}::*luxAB*
Rlu/OD_{595nm}
**

Figure 1. Expression of transcription reporter fusions of *tdhA* (A, B) and *tdhS* (C, D) under oxidative stress conditions. Wild-type *V. parahaemolyticus* carrying the *tdhA-luxAB* or *tdhS-luxAB* transcription fusion were grown in LBS medium supplemented with 3 μg/ml tetracycline. Oxidative stresses against *V. parahaemolyticus* were applied by including 0.1 mM hydrogen peroxide (A for *tdhA-luxAB*; C for *tdhS-luxAB*) or 0.1 mM paraquat (B for *tdhA-luxAB*; D for *tdhS-luxAB*) to cultures at the early exponential stage (OD_{595}= 0.6). Luminescence produced by each strain was determined using a luminometer during the whole growth period. The specific luciferase activities were presented by plotting the normalized values as relative light units (RLU) per biomass (OD_{595}).

2. Effect of iron availability on the level of *tdh* expressions

The second environmental condition tested as a modulator for *tdh* expression was iron concentration. To achieve the iron-limiting conditions, 200 μM 2,2'-dipyridyl or 20 μM ethylenediamine-*N*,*N*'-diacetic acid (EDDA) was added to the cultures of *V. parahaemolyticus* carrying *tdhA::luxAB* (Fig. 2A and 2B, respectively). Inclusion of 2,2'-dipyridyl induced a threefold increase of luciferase activity of *tdhA::luxAB* fusion, whereas addition of EDDA did not trigger any change in expression of the same fusion. The presence of 2,2'-dipyridyl affected the growth of *V. parahaemolyticus* after the exponential phases were compared with untreated bacteria (Fig. 2A and 2C). In the same manner, luciferase activity of *tdhS::luxAB* fusion increased about threefold with 2,2'-dipyridyl, but not with EDDA (Fig. 2C and 2D, respectively). Bacterial growth was not affected by EDDA (Fig. 2B and 2D).

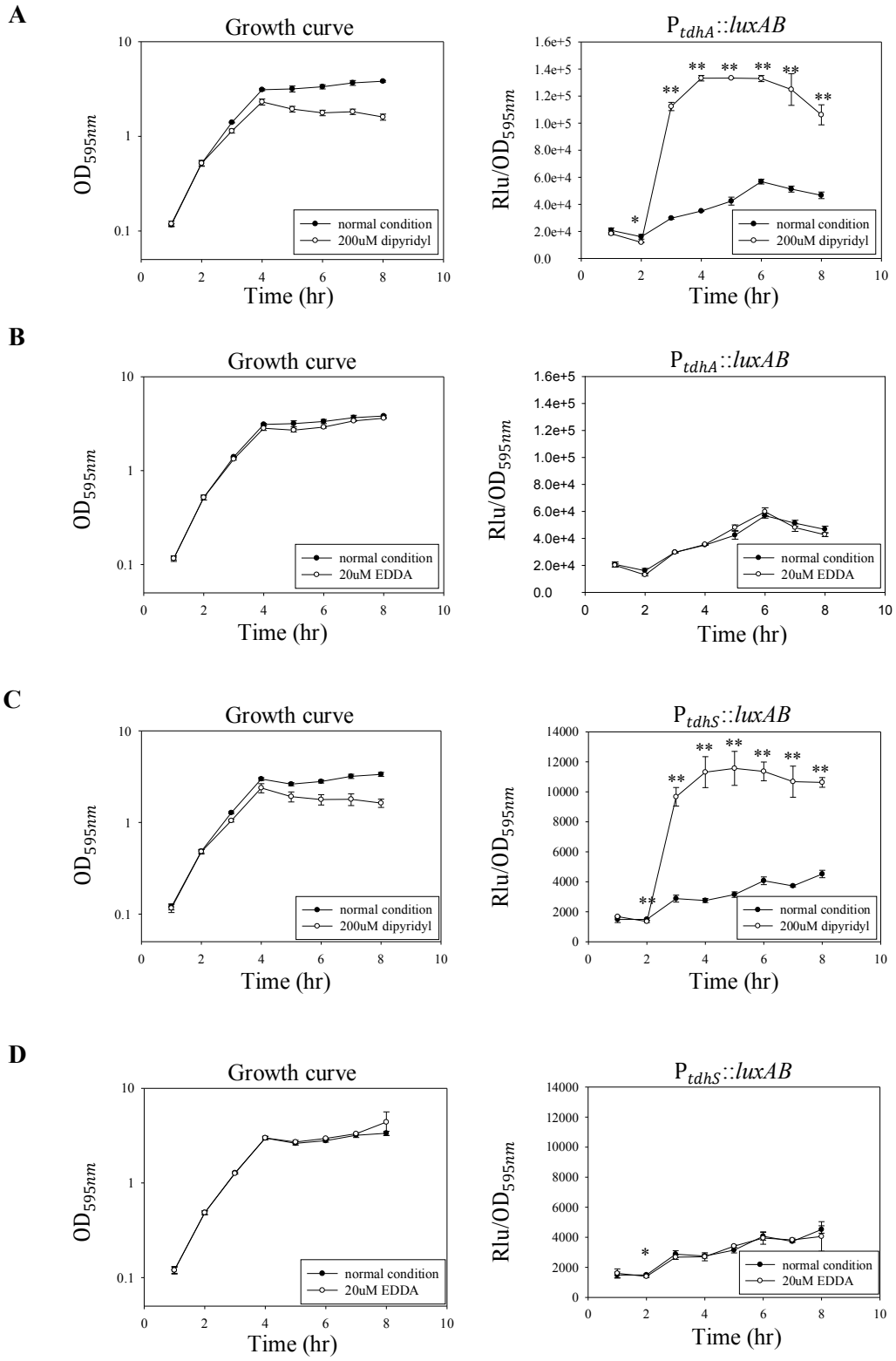
A
Growth curve
OD_{595nm}
Time (hr)
normal condition
200uM dipyridyl
P_{tdhA}::*luxAB*
Rlu/OD_{595nm}
Time (hr)
normal condition
200uM dipyridyl
B
Growth curve
OD_{595nm}
Time (hr)
normal condition
20uM EDDA
P_{tdhA}::*luxAB*
Rlu/OD_{595nm}
Time (hr)
normal condition
20uM EDDA
C
Growth curve
OD_{595nm}
Time (hr)
normal condition
200uM dipyridyl
P_{tdhS}::*luxAB*
Rlu/OD_{595nm}
Time (hr)
normal condition
200uM dipyridyl
D
Growth curve
OD_{595nm}
Time (hr)
normal condition
20uM EDDA
P_{tdhS}::*luxAB*
Rlu/OD_{595nm}
Time (hr)
normal condition
20uM EDDA

Figure 2. Effect of iron availability on expression of transcription reporter fusions of *tdhA* (A, B) and *tdhS* (C, D). Wild-type *V. parahaemolyticus* carrying the *tdhA-luxAB* or *tdhS-luxAB* transcription fusion was grown in LBS medium supplemented with 3 μg/ml tetracycline. Iron-depleted conditions were prepared by adding 200 μM 2,2'-dipyridyl (A for *tdhA-luxAB*; C for *tdhS-luxAB*) or 20 μM ethylenediamine-*N*,*N*′-diacetic acid (B for *tdhA-luxAB*; D for *tdhS-luxAB*) to bacterial culture at the early exponential stage (OD_{595} = 0.6). Luminescence produced by each strain was determined using a luminometer during the whole growth period. The specific luciferase activities were presented by plotting the normalized values as relative light units (RLU) per biomass (OD_{595}).

3. Role of ferric uptake regulator (Fur) and iron sulfur cluster regulator (IscR) in *tdhA* expression

The increase of *tdhA::luxAB* expression with 2,2'-dipyridyl suggested the presence of transcription factor (s) involved in iron control of *tdhA* expression. Two candidate regulators are ferric uptake regulator (*fur*) and iron-sulfur cluster regulator (*iscR*). Fur is a small protein that complexes with iron and regulates expression of multiple genes by binding to conserved sequences called Fur boxes[49]. IscR functions as a sensor of oxidative state of Fe-S clusters and modulates biogenesis of the Fe-S clusters[35]. Most importantly, the *fur*-deficient mutant *V. parahaemolyticus* was made by deleting the *fur* gene from its chromosome. Deletion of the *fur* gene in a chromosome of the mutant *V. parahaemolyticus* was confirmed by PCR using primers, fur-upF and fur-downR (Fig. 3A). While wild-type *V. parahaemolyticus* with an intact *fur* gene produced a 1.9-kb-long DNA fragment, PCR with the *fur* mutant *V. parahaemolyticus* produced a larger 2.6-kb DNA fragment due to the insertion of the kanamycin-resistant *nptI* gene. Expression of *tdhA::luxAB* in the *Δfur* mutant was similar to that of the wild-type (Fig. 3B). Addition of an iron chelator also resulted in an increase of luciferase activity of *tdhA::luxAB* fusion in the *Δfur* mutant as shown in wild-type *V parahaemolyticus*. This result clearly indicates that Fur is not the regulator mediating transcriptional activation of the *tdhA* gene under iron-limited conditions.

The role of IscR in iron control of *tdh* expression was also observed by constructing the *ΔiscR* mutant. Deletion of the *iscR* gene was also confirmed by

PCR using primers, iscR-upF and iscR-downR (Fig. 4A). While wild-type *V. parahaemolyticus* with intact *iscR* gene produced a 2.9-kb-long DNA fragment, the PCR product derived from the *ΔiscR* mutant *V. parahaemolyticus* was 1.7 kb long. *tdhA* expression in wild-type and *ΔiscR* mutants was not different under normal conditions. When 2,2'-dipyridyl was added to the culture, the *ΔiscR* mutant also showed an increase in luciferase activity of *tdhA::luxAB* fusion (Fig. 4B). These results indicate that IscR is not responsible for iron control of *tdhA* expression, and suggest the presence of another regulatory transcription factor(s) of *tdhA* gene under iron-depleted conditions.

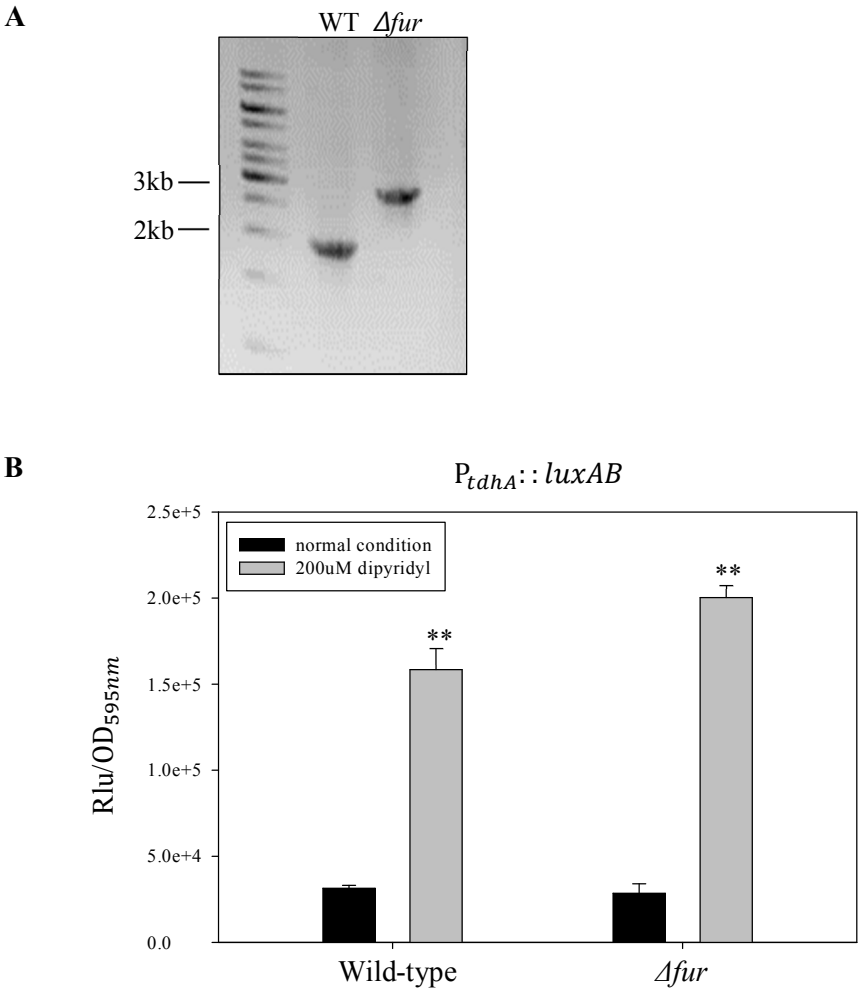

Figure 3. Role of Fur in *tdhA* gene expression. A - Construction of *V. parahaemolyticus* mutant defective in *fur* using two sets of primers (Table 2) to delete VP0833. Deletion of the corresponding gene was examined by PCR using a pair of primers, fur-upF and fur-downR; B - Expression of a transcription reporter fusion of *tdhA*. Light production was determined by adding 200 μM 2,2'-dipyridyl. The specific luciferase activities were presented as described in Fig. 1.

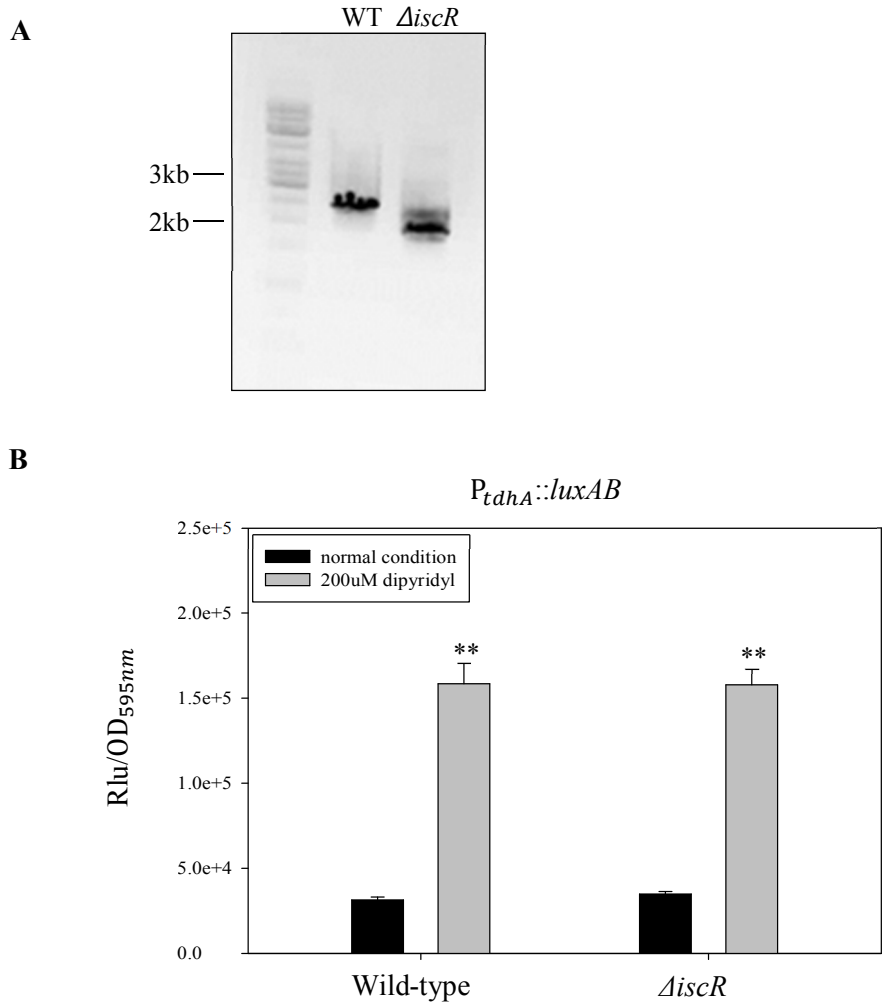

Figure 4. Role of IscR in *tdhA* gene expression. A - Construction of *V. parahaemolyticus* mutant defective in *iscR* using two sets of primers (Table 2) to delete VP0595. Deletion of the corresponding gene was examined by PCR using a pair of primers, iscR-upF and iscR-downR; B - Expression of a transcription reporter fusion of *tdhA*. Light production was determined by adding 200 μM 2,2'-dipyridyl. The specific luciferase activities were presented as described in Fig. 1.

4. Effect of bile on *tdhA* expression

Bile secreted by the gallbladder performs pleiotropic roles in human intestine, and one of its functions may be to protect the host against enteric pathogens[50]. Therefore, enteric pathogens such as *V. parahaemolyticus* are evolved to adapt to or cope with bile or bile salt. Bile acids, as a mixture of the sodium salts of taurocholic, glycocholic, deoxycholic, chenodeoxycholic, and cholic acid, are major components of crude bile. As the third environmental factor for *tdh* expression, crude bile or bile salt was added to *V. parahaemolyticus* carrying the *tdhA::luxAB* fusion plasmid to examine its role in expression of *tdh* genes (Fig. 5). Addition of crude bile increased expression of *tdhA::luxAB* fusion about sixfold, whereas the effect of bile salts was smaller (less than threefold) (Fig. 5A and 5B, respectively). For *V. parahaemolyticus* carrying the *tdhS::luxAB* fusion plasmid, luciferase activity increased only with addition of crude bile (ninefold), but not with bile salts (Fig. 5C and 5D, respectively). This data indicate that crude bile induced expression of both *tdhA* and *tdhS*.

The next experiment aimed to identify transcription factor(s) activating *tdhA* expression in the presence of bile. Therefore, we performed a ligand fishing experiment (Fig. 6). Two different lysates, *V. parahaemolyticus* grown in the absence (lane 3) or the presence of 0.05% crude bile (lane 4), were passed through the column coupled with a promoter region of the *tdhA* gene. As a control, *V. parahaemolyticus* grown in the presence of 0.05% crude bile was also passed

through the other column coupled to DNA encoding a portion of TdhA (lane 2). SDS-PAGE of these bound proteins revealed three candidate protein bands, which specifically bound to the *tdhA* promoter, but not to the *tdhA* coding region, and the amount of bound proteins increased in the lysates prepared from bacteria grown with crude bile. Three protein bands were excised from the gel and analyzed by LC MS/MS, and identified as phage shock protein (psp) operon transcription regulator (38-kDa, VP1172), a putative transcriptional regulator LysR family (35-kDa, VPA1607), and copper-sensing two-component system response regulator CusR (25-kDa, VPA0919).

A

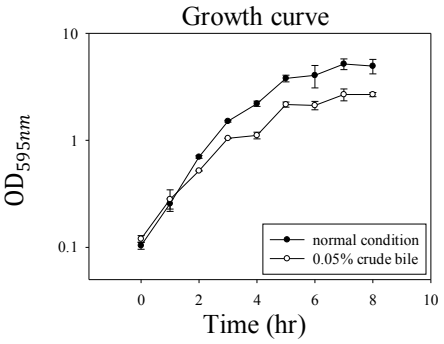
Growth curve
OD_{595nm}
Time (hr)
normal condition
0.05% crude bile

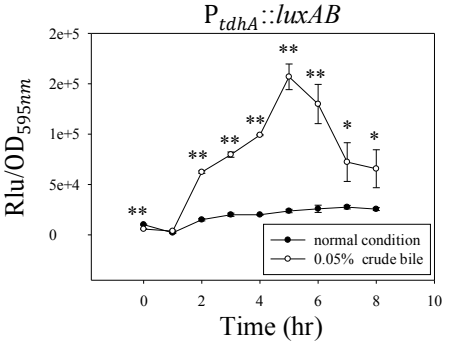
P_{tdhA}::*luxAB*
Rlu/OD_{595nm}
Time (hr)
normal condition
0.05% crude bile

B

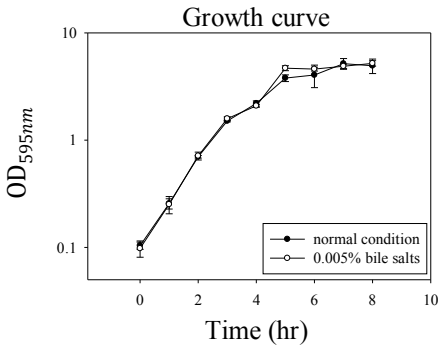
Growth curve
OD_{595nm}
Time (hr)
normal condition
0.005% bile salts

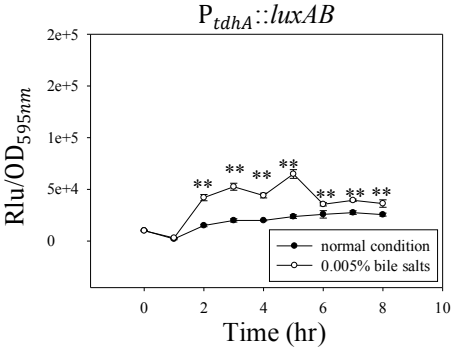
P_{tdhA}::*luxAB*
Rlu/OD_{595nm}
Time (hr)
normal condition
0.005% bile salts

C

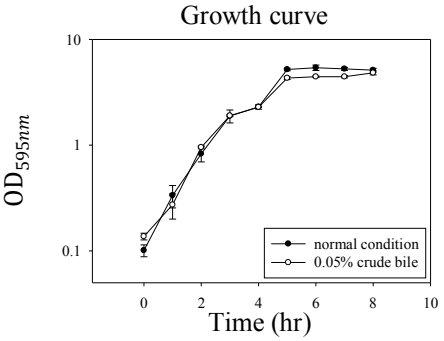
Growth curve
OD_{595nm}
Time (hr)
normal condition
0.05% crude bile

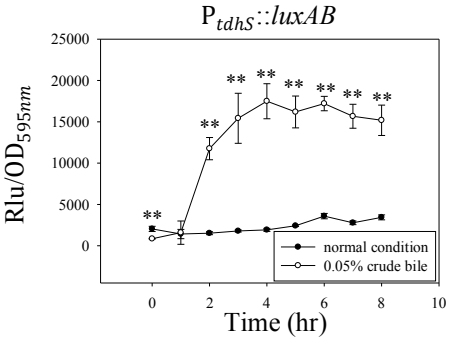
P_{tdhS}::*luxAB*
Rlu/OD_{595nm}
Time (hr)
normal condition
0.05% crude bile

D

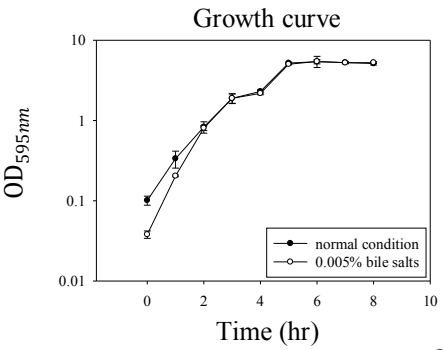
Growth curve
OD_{595nm}
Time (hr)
normal condition
0.005% bile salts

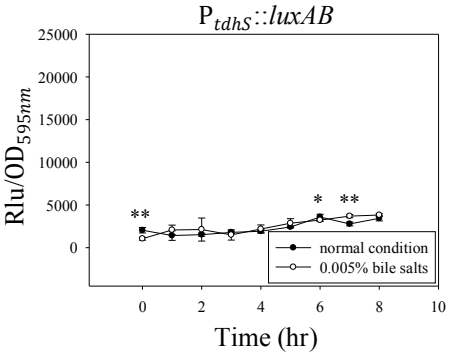
P_{tdhS}::*luxAB*
Rlu/OD_{595nm}
Time (hr)
normal condition
0.005% bile salts

Figure 5. Effect of crude bile or bile salts on expression of transcription reporter fusions of *tdhA* (A, B) and *tdhS* (C, D). Wild-type *V. parahaemolyticus* carrying the *tdhA-luxAB* or *tdhS-luxAB* transcription fusion was grown in LBS medium supplemented with 3 μg/ml tetracycline. These cells were grown in the presence of 0.05% (wt/vol) crude bile (A for *tdhA-luxAB*; C for *tdhS-luxAB*) or 0.005% (wt/vol) bile salt (B for *tdhA-luxAB*; D for *tdhS-luxAB*). Luminescence produced by each strain was determined using a luminometer during the whole growth period. The specific luciferase activities were presented by plotting the normalized values as relative light units (RLU) per biomass (OD_{595}).

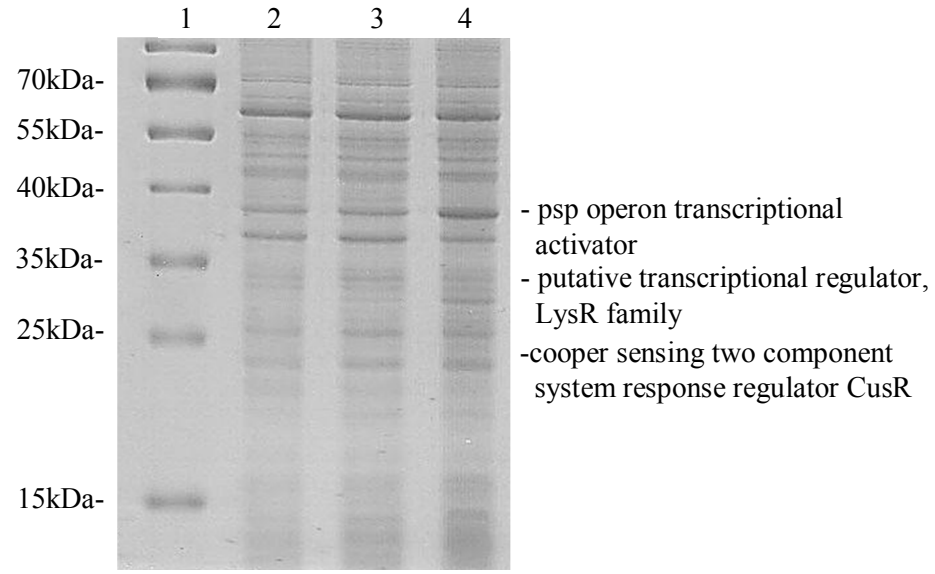

Figure 6. Ligand fishing experiment to find proteins associated with *tdhA* promoter. A bait DNA fragment contained the 468-bp promoter of the *tdhA* gene (lanes 3 and 4). A 500-bp coding region of TdhA was used as a control DNA (lane 2). Wild-type *V. parahaemolyticus* grown in the presence or absence of 0.05% (wt/vol) crude bile was lysed and loaded on to the column immobilized either with the *tdhA* promoter or control DNA fragment. Ten micrograms of the eluted protein was analyzed by SDS-PAGE. Protein bands appearing only in the column coupled to *tdhA* promoter DNA were excised, and analyzed by quadrupole TOF (Q-TOF) in addition to MALDI-TOF MS. For the Q-TOF liquid chromatography-tandem MS (LC-MS/MS) data sets, tandem mass spectra were submitted to our MASCOT in-house database search engine (Vibrio DB).

5. Role of ToxR in *tdhA* expression induced by crude bile

ToxR was identified as a transcription regulator of virulence factors including transcription factor ToxT, cholera toxin (CT), and toxin-coregulated pilus (tcp) in *V. cholerae* (Fig. 7). It has been reported in *V. cholerae* that ToxR is also involved in bile-induced expression of outer membrane protein, OmpU[40,41,42]. Thus, the role of ToxR in bile-induced *tdhA* expression was examined in *V. parahaemolyticus* by constructing ToxR-deficient mutant *V. parahaemolyticus* (Fig. 8A). Deletion of the *toxR* gene in a chromosome of the mutant *V. parahaemolyticus* was confirmed by PCR using primers, toxR-upF and toxR-downR. PCR with wild-type *V. parahaemolyticus* produced a DNA fragment of 2.3 kb, whereas the PCR product of the *toxR* mutant *V. parahaemolyticus* was a DNA fragment of 2.6 kb, which includes the *nptI* gene. A plasmid containing the *tdhA*::*luxAB* fusion was transferred into the *ΔtoxR* mutant *V. parahaemolyticus* via conjugation. Under normal conditions, i.e., in the absence of crude bile, *tdhA* expression was barely different between the wild-type and *ΔtoxR* mutant (Fig. 8B). In contrast with wild-type cells, activity of *tdhA::luxAB* was not induced with crude bile in *toxR* mutant. This result indicated that ToxR regulates the bile-induced expression of the *tdhA* gene.

Involvement of ToxR in bile-induced expression of the *tdhA* gene was also confirmed by Western blot analysis using anti-TdhA antibodies (Fig. 8C). The culture supernatants were prepared from *V. parahaemolyticus* strains grown in LBS broth in the absence or presence of 0.05% crude bile and used for Western blot analysis. The amount of TdhA was increased by crude bile in the secretome of wild-

type, whereas the amount of secreted TdhA was not changed in the *ΔtoxR* mutant by crude bile. As a control, the amount of OmpU (a well-known target protein of ToxR) was also examined in the *ΔtoxR* mutant, which was found to be defective in expression of OmpU. The level of FlaA, flagellin, was also monitored as a loading control for the secreted proteins.

The next experiment aimed to find whether ToxR regulates *tdhA* transcription via direct binding to the *tdhA* promoter region. In *V. cholerae*, two distinct modes of the ToxR-mediated control are known, which occur in a ToxT-dependent manner or via direct binding by ToxR. Because *V. parahaemolyticus* has no *toxT* gene, we thought that regulation of *tdhA* is controlled directly by binding of ToxR. ToxR is an integral membrane protein, consists of 294 amino acids, and has three functional domains: N-terminus cytoplasmic domain, short transmembrane domain, and C-terminus periplasmic domain. The cytoplasmic domain of the ToxR binds directly to a repeated TTTTGAT motif in the cholera toxin promoter[51]. A homology search between *V. parahaemolyticus* ToxR and *V. cholerae* ToxR revealed the tentative cytoplasmic DNA binding domain as shown in Fig. 9A. Recombinant protein encoding the N-terminus ToxR cytoplasmic region was expressed as a histidine-tagged form in the *E. coli* system, and purified by affinity chromatography (Fig. 9B). A gel-shift assay was performed using recombinant truncated ToxR protein (rcToxR) and a 234-bp DNA fragment including an upstream region of the *tdhA* gene (Fig. 9C). Addition of rcToxR resulted in retarded mobility of the DNA fragment due to complex formation of rcToxR and probe DNA, in an rcToxR dose-

dependent manner. Binding of rcToxR to the DNA was found to be specific, because increase of excess unlabeled DNA abolished the retarded bands.

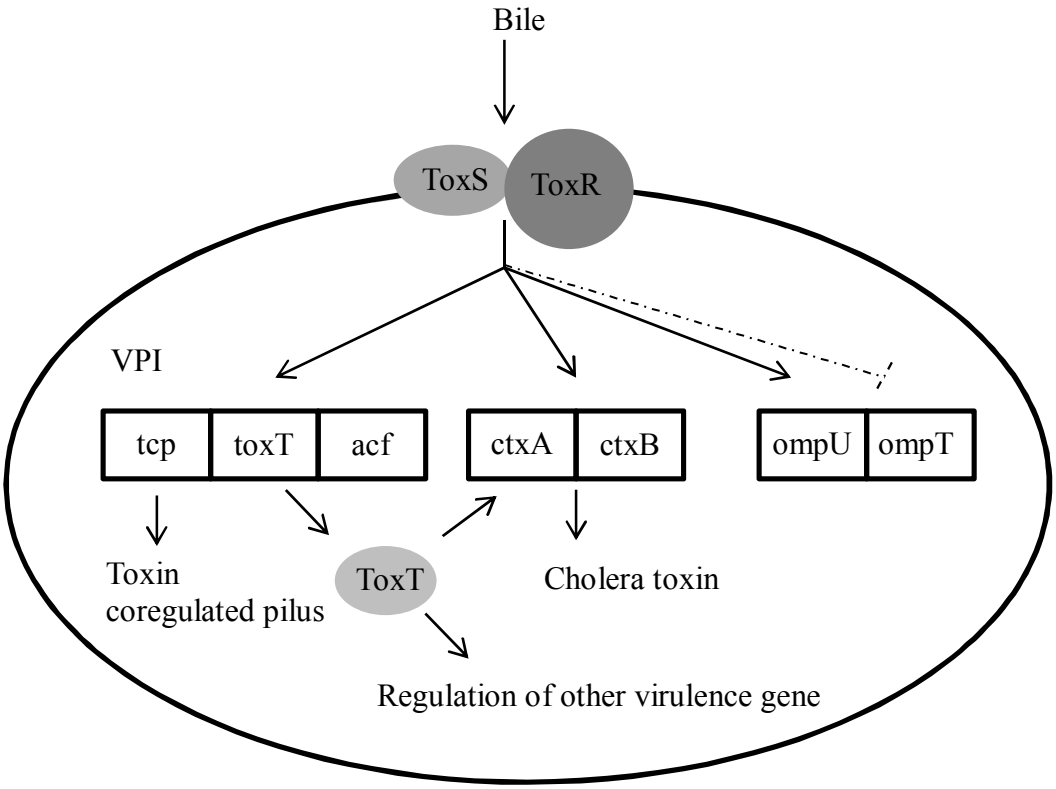

Figure 7. Role of ToxR in bile-induced transcription in *V. cholerae*. In *V. cholerae*, bile-induced transcription of various genes encoding virulence factors (toxin coregulated pilus and cholera toxin subunits) and outermembrane proteins (OmpU and OmpT) occurs through two-component signal transduction system, ToxRS. In addition, bile also activates transcription of another transcription factor, ToxT, which also involves expression of other virulence factors.

A

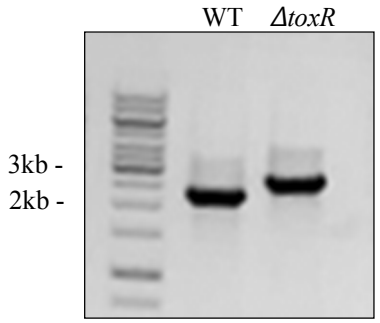
WT
ΔtoxR
3kb -
2kb -

B

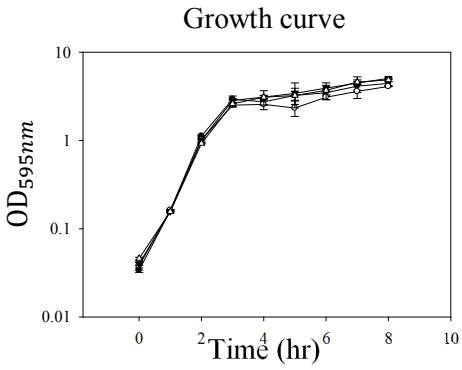
Growth curve
OD_{595nm}
10
1
0.1
0.01
0
2
4
6
8
10
Time (hr)

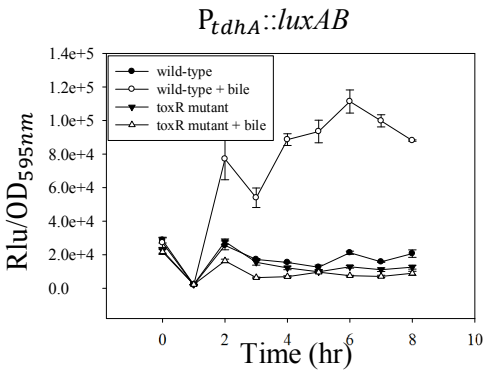
P_{tdhA}::luxAB
Rlu/OD_{595nm}
1.4e+5
1.2e+5
1.0e+5
8.0e+4
6.0e+4
4.0e+4
2.0e+4
0.0
wild-type
wild-type + bile
toxR mutant
toxR mutant + bile
0
2
4
6
8
10
Time (hr)

C

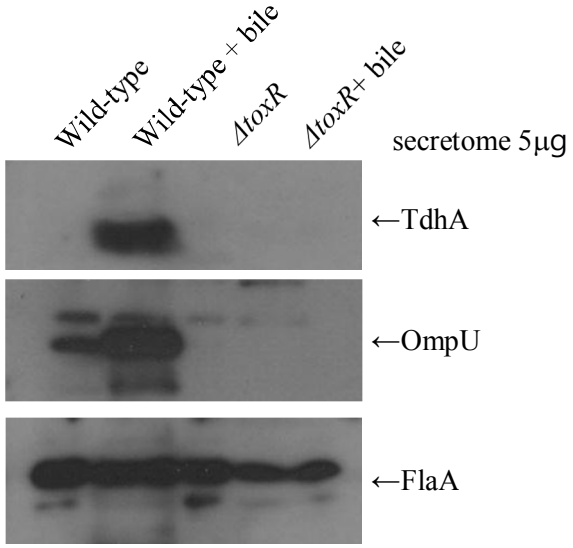
Wild-type
Wild-type + bile
ΔtoxR
ΔtoxR+ bile
secretome 5μg
←TdhA
←OmpU
←FlaA

Figure 8. Role of ToxR in *tdhA* gene expression. A - Construction of *V. parahaemolyticus* mutant defective in *toxR* using two sets of primers (Table 2) to delete VP0820. Deletion of the corresponding gene was examined by PCR using a pair of primers, toxR-upF and toxR-downR; B - Expression of a transcription reporter fusion of *tdhA*. The specific luciferase activities were presented as described in Fig. 1; C – Western blot analysis of secretomes using anti-TdhA antibodies. Secreted proteins were prepared from wild-type and *ΔtoxR* mutant *V. parahaemolyticus* strains grown in the absence and in the presence of crude bile (0.05%). These secretomes were also monitored for OmpU and FlaA levels by Western blot analysis using anti-OmpU antibodies and anti-FlaA antibodies, respectively.

A

MTNIGTKFLLAQRFTFDPNSNSLADQQSGNEVVRLGSNESRIL
LMLAERPNEVLTRNELHEFVWREQGFEVDDSSLTQAISTLRK
MLKDSTKSPEFVKTVPKRGYQLICTVERLSPLSSDSSSIEVEEP
ASDNNDASANEVETIVEPSLATTSDAIVEPEAPVVPEKAPVAS
AVNPWIPRVILFLALLLPICVLLFTNPAESQFRQIGEYQNVPVM
TPVNHPQINNWLPSIEQCIERYVKHHAEDSLPVEVIATGGQN
NQLILNYIHDSNHSYENVTLRIFAGQNDPTDICK

B

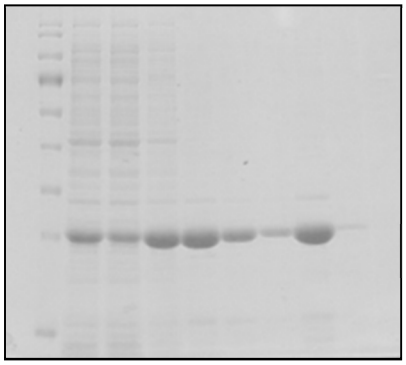

1 lane ; size marker
2 lane ; lysate
3 lane ; flow through
4 lane ; wash 1
5 lane ; wash 2
6 lane ; elution 1
7 lane ; elution 2
8 lane ; elution 3
9 lane ; elution 4

C

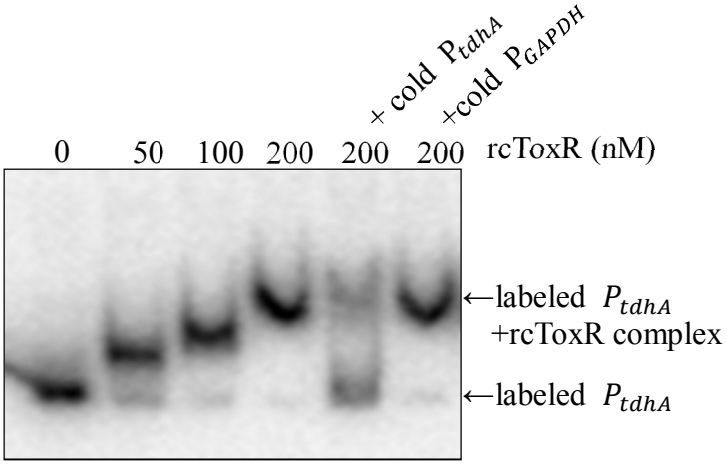

Figure 9. Formation of recombinant ToxR protein containing cytoplasmic domain and its interaction with *tdhA* promoter region. A - Putative amino acid sequence of *V. parahaemolyticus* ToxR. Based on the information on *V. cholerae* ToxR, the N-terminal portion of the protein (underlined) was predicted to be present on the cytoplasmic side of the bacterial cells where this region binds to the promoters of the target genes; B - Formation of *V. parahaemolyticus* recombinant cytoplasmic ToxR (rcToxR). rcToxR was expressed in *E. coli* with histidine tags, purified using Talon affinity chromatography, and then subjected to 12% SDS-PAGE; C - Gel-shift assay for binding of rcToxR to the regulatory region of *tdhA*. A labeled 234-bp DNA fragment including upstream region of *tdhA* was incubated with various concentrations of rcToxR (0 ~ 200 μM). The reaction mixtures were separated on 6% non-denaturing polyacrylamide gel. For competition analysis, the unlabeled DNA fragments were included in the reactions at a concentration of 1 μM.

6. rTdhA induces necroptosis in human cell lines

Besides the expression pattern of Tdhs, the role of TdhA was investigated with respect to its action on the host cells in this study. Tdh has been reported to have hemolytic activity, cytotoxicity, and enterotoxicity[17,18,19]. Attenuation of mouse lethality of *Δtdh* mutants indicated that Tdh is a major virulence factor of *V. parahaemolyticus*[52]. Most of all, recombinant TdhA (rTdhA) protein was prepared in order to study its role in interaction with the host cells. Examination of the putative amino acid sequence of TdhA protein revealed that this protein has a signal peptide, an indication of being secreted out from the bacterial cells (Fig. 10A). A cleavage site of the signal peptide was predicted at the 24th amino acid of the putative amino acid sequence of TdhA.

To obtain secreted rTdhA protein, an *E. coli-V. parahaemolyticus* shuttle plasmid, pRK415, was used to make the rTdhA-expression system functioning in *V. parahaemolyticus*. Expression of rTdhA was induced with IPTG and crude bile (Fig. 10B). As shown by SDS-PAGE, a larger amount of rTdhA protein was produced by crude bile, as expected. rTdhA protein was also confirmed using anti-His antibodies by Western blot analysis. Therefore, rTdhA protein used in this study was prepared from culture supernatants of *V. parahaemolyticus* grown in the presence of crude bile. After rTdhA was purified from the *V. parahaemolyticus* culture supernatant via affinity chromatography, it was incubated with the human cell line, HT-29. Most of all, rTdhA-treated cells were monitored for morphological changes under transmission electron microscopy (Fig. 11). At 3 hr after exposure to rTdhA (0.5 or

2 μM), HT-29 cells showed dramatic morphological changes, which have been previously described in dying cells[53]. For example, loss of membrane integrity, membrane blebbing, appearance of vacuoles, and cell lysis were discernible in the rTdhA-treated cells.

To characterize the cytotoxicity induced by *V. parahaemolyticus* rTdhA, rTdhA-treated HT-29 cells were stained with Annexin V and propidium iodide (PI), indicative of apoptotic cells and necrotic cells, respectively (Fig. 12). Upon treatment with rTdhA, HT-29 cells were found to be stained with both Annexin V and PI. HT-29 cells treated with staurosporin (STS) were included as an apoptosis inducer, which showed strong staining with Annexin V, as expected. A larger number of HT-29 cells was stained with PI than Annexin V, suggesting that rTdhA-induced cell death has characteristics similar to necrosis.

In addition to florescence microscopy, HT-29 cells stained with Annexin V and PI were examined by flow cytometry analysis (Fig. 13). In the case of HT-29 cells treated with 2 μM rTdhA, the degree of Annexin V and PI staining was gradually increased in a time-dependent manner. 5% of HT-29 cells were stained with Annexin V and PI in the absence of rTdhA. HT-29 cells increased by up to 28% in 6 hr. HT-29 cells exposed to 10 mM hydrogen peroxide for 3 hr were included as a positive control and resulted in 27.9% cells stained by Annexin V and PI.

To investigate whether rTdhA-mediated cell death is related to necroptosis, necrostatin-1 (Nec-1), a chemical compound inhibiting the kinase activity of receptor-interacting protein-1 (RIP-1) involved in necroptosis, was applied to HT-29

cells prior to rTdhA treatment (Fig. 14). Pretreatment of HT-29 with Nec-1 resulted in a decrease of lactate dehydrogenase (LDH) release by rTdhA-treated cells. LDH release from HT-29 cells without rTdhA treatment was 7% and 9% in the absence and presence of Nec-1 pretreatment, respectively. LDH release increased with rTdhA in a dose-dependent manner (from 26% to 42%). Pretreatment with Nec-1 resulted in a decrease of LDH release from HT-29 cells treated with various concentrations of rTdhA. This result indicates RIP1-mediated necroptosis is one of the pathways involved in the rTdhA-mediated cell death.

A

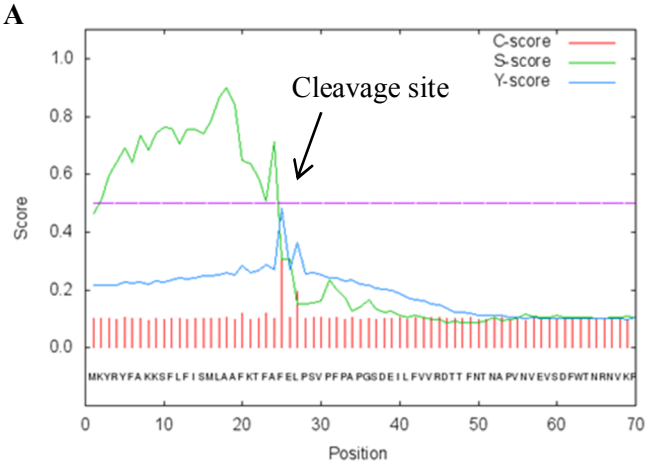

B

Coomassie staining

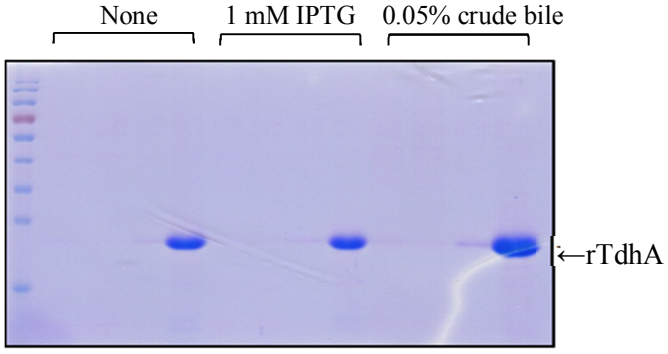

Anti-His

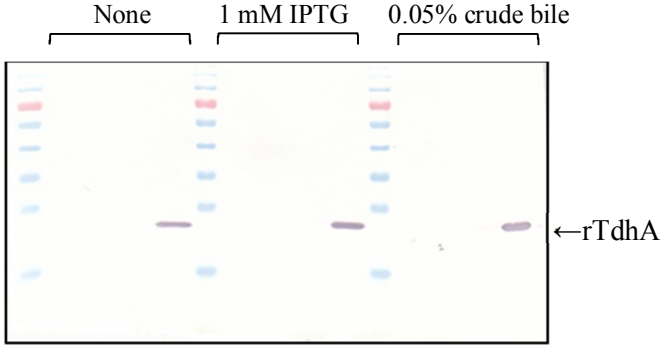

Figure 10. Overexpression of recombinant TdhA (rTdhA) from culture supernatants of *V. parahaemolyticus.* A - A putative signal peptide of TdhA was predicted by the program SignalP 4.1 server; B – Overexpression and purification of TdhA from *V. parahaemolyticus*. rTdhA was prepared from *V. parahaemolyticus* carrying pRKtdhA, which was grown in LBS broth at 37°C in the presence of 0.05% crude bile. Supernatants were passed through Talon affinity chromatography system, and the purified proteins were loaded into 12% SDS-PAGE.

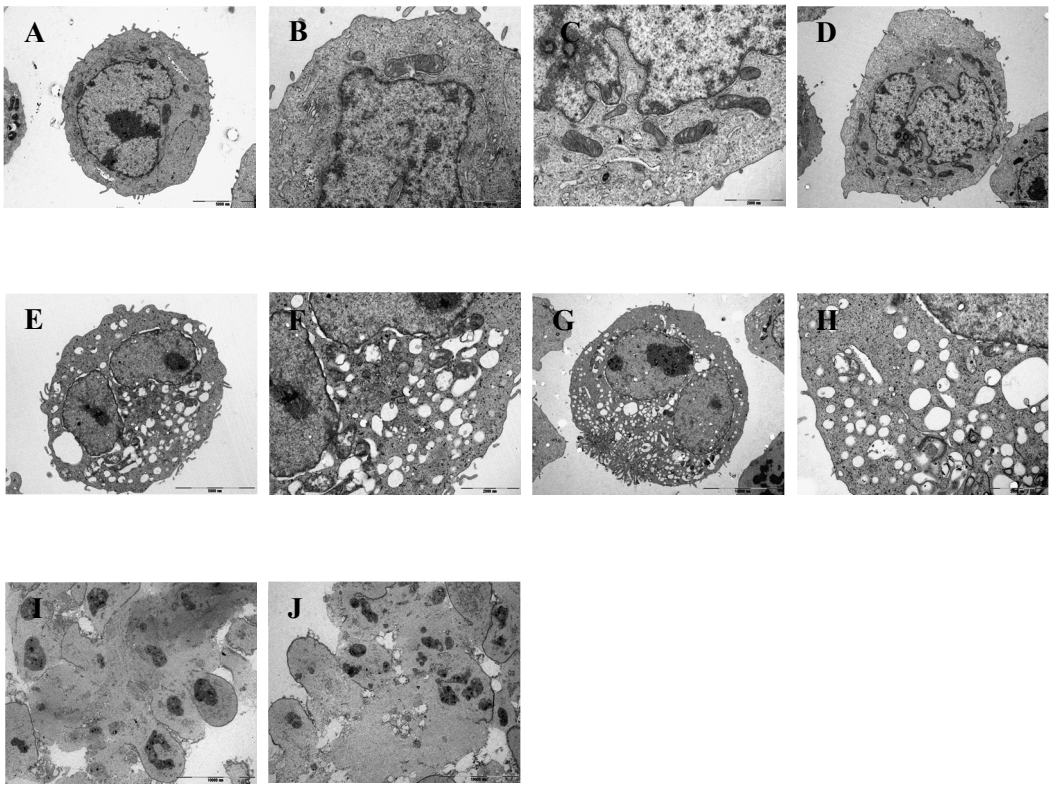

Figure 11. Morphologic observation of HT-29 cells treated by rTdhA via transmission electron microscopy (TEM). HT-29 cells (2×10^5) were seeded in a 24-well plate and incubated at 37°C for 24 hr in a 5% CO_2 incubator. At 70% confluence, prepared cells were treated with 0.5 μM or 2 μM rTdhA. The harvested cells were fixed with 2% glutaraldehyde/2% paraformaldehyde solution, and then embedded in paraffin. The sections of the prepared cells were observed under a TEM. (A), (B), (C) and (D); absence of rTdhA; (E), (F), (G) and (H), treated with 0.5 μM TdhA; (I) and (J), treated with 2 μM TdhA.

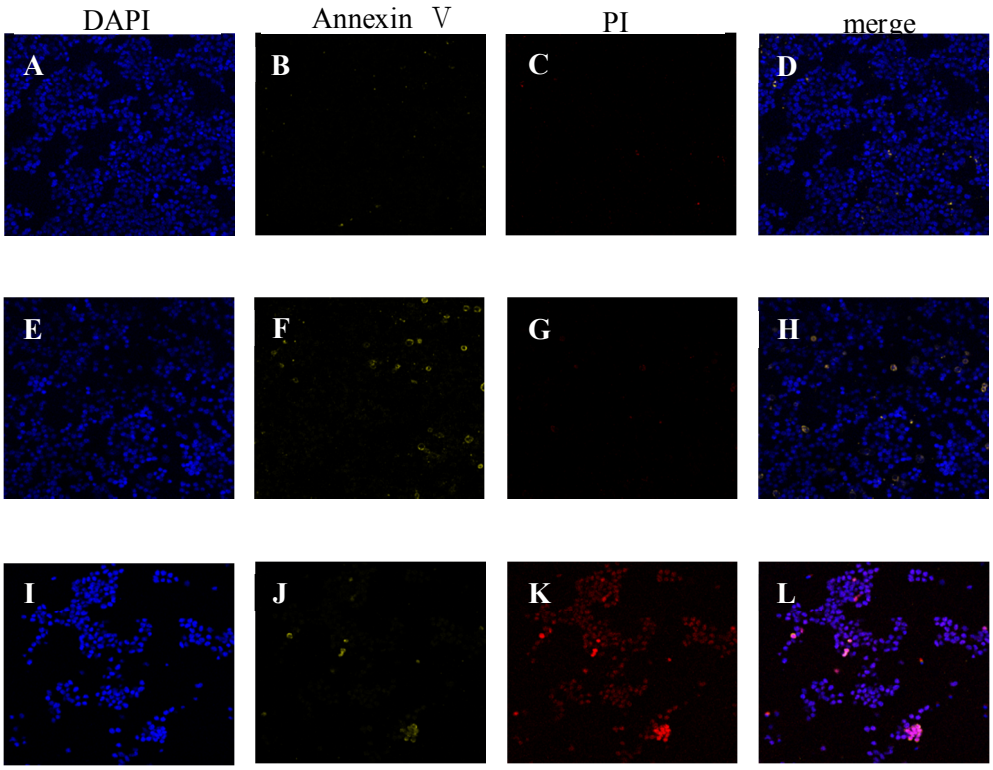

Figure 12. Annexin V and PI staining of rTdhA-treated HT-29 cells. 2 X 10^5 HT-29 cells were treated with rTdhA for 3 hr and stained with DAPI (blue), Annexin V-FITC (yellow) and propidium iodide (PI, red), and then observed under confocal microscopy. Panels A, B, C, and D, HT-29 cells without treatment; panels E, F, G, and H, HT-29 cells incubated with 2 μM staurosporin as a positive control; panels I, J, K, and L, HT-29 cells incubated with 1.5 μM rTdhA.

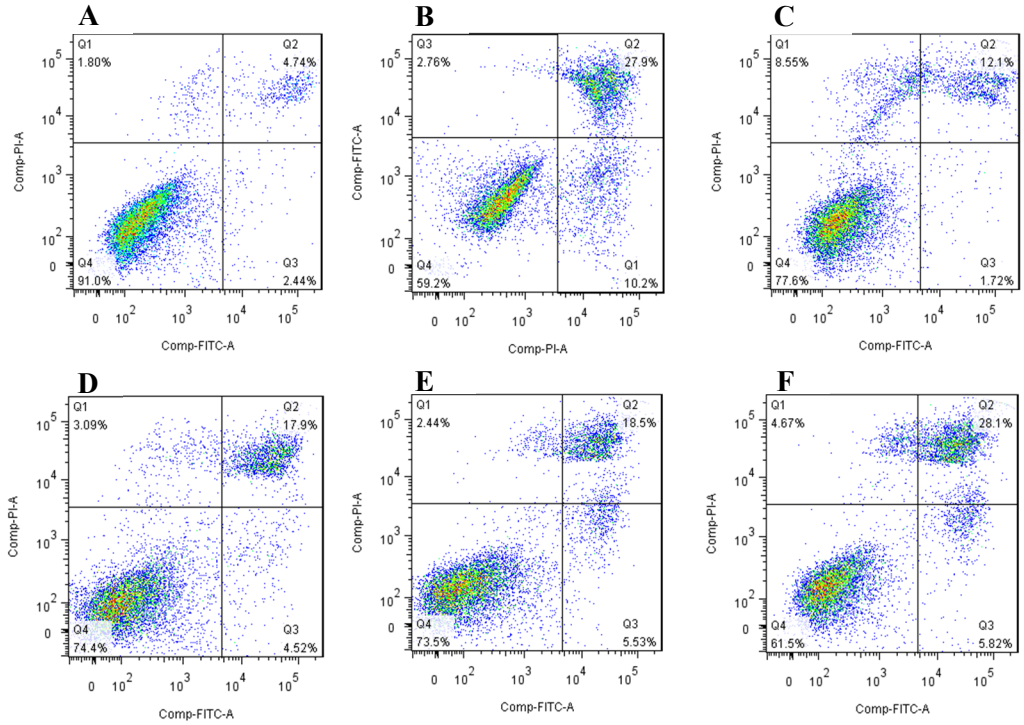

Figure 13. Flow cytometric measurement of cell death induced by rTdhA. 2 X 10^5 HT-29 cells were seeded in a 24-well plate. After starvation with FBS-free DMEM medium, the cells were treated with 2 μM rTdhA for various periods (from 30 min to 6 hr) at 37°C. Then, cells were stained with Annexin V and PI at a final concentration of 1.0 mg/ml. The degree of binding was assessed using fluorescence-activated cell sorting (FACS) analysis. FACS analyses were performed on at least 10,000 cells per sample with a FACScan (Becton Dickinson). Panel A, untreated HT-29 cells; panel B, HT-29 cells treated with 20 mM hydrogen peroxide as a positive control of cell death; panels C, D, E, and F, HT-29 cells treated with rTdhA and incubated for 30 min, 1, 3, and 6 hrs, respectively.

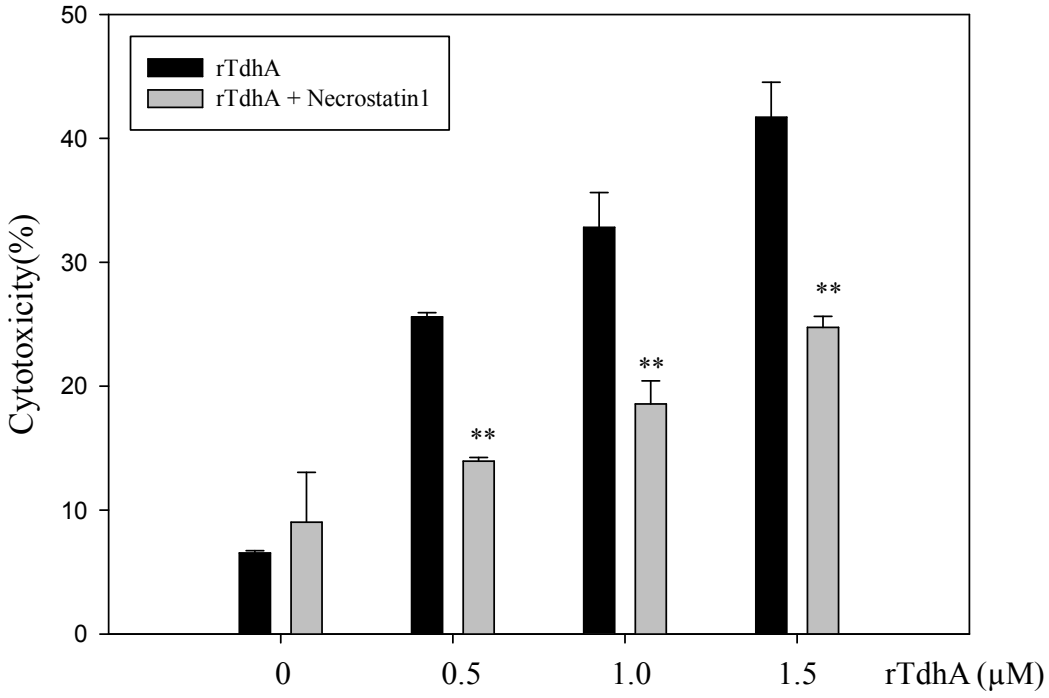

Figure 14. Inhibition of rTdhA-induced cytotoxicity by necrostatin-1. 3×10^4 HT-29 cells were pretreated with 1% DMSO solution containing 50 μM Necrostatin-1 for 1 hr, and then exposed to rTdhA for 3 hr at 37°C. Degree of cytotoxicity of rTdhA was monitored by relative lactate dehydrogenase release, using CytoTox96® Assay Kit (Promega). As a control, a separate sample of HT-29 cells was pretreated with 1% DMSO prior to treatment with rTdhA.

IV. DISCUSSION

V. parahaemolyticus has been recognized as an agent of gastroenteritis and is associated with consumption of seafood, but not all strains of this species are pathogenic. A marker for pathogenic *V. parahaemolyticus* is beta-type hemolysis on a special blood agar medium, Wagatsuma's agar[54,55]. Thus, this particular hemolysin, thermostable direct hemolysin (Tdh), has been the subject of extensive study[56,57,58]. This study aimed 1) to investigate how expression of Tdh varies under diverse stressed conditions, and 2) to understand the cytotoxic activity of Tdh against human cell lines using recombinant Tdh (rTdh).

Genomic data on *V. parahaemolyticus* indicated the presence of two genes, *tdhA* and *tdhS*, encoding Tdh[59]. The expression level from the presumed promoter of the *tdh*A gene was 20-fold higher than that of the *tdh*S promoter in *E. coli*[60,61]. Many bacteria have evolved survival mechanisms against diverse stresses, such as starvation, temperature fluctuation, oxidative stress, and osmotic shock[62,63]. In this study, transcription of two *tdh* genes was monitored in *V. parahaemolyticus* under various environmental conditions. To find the role of reactive oxygen species (ROS) in *tdhA* and *tdhS* expression, bacterial cells carrying the *tdh::luxAB* fusion were treated with hydrogen peroxide or paraquat (Fig. 1). As expected, the expression level of *tdhA* was tenfold higher than *tdhS* under normal conditions. Under oxidative stressed conditions, both the growth of *V. parahaemolyticus* and the expression of two *tdh* genes were not affected.

The second possible modulator for *tdh* expression was iron concentration. Iron availability was found as a modulator for virulence of *V. vulnificus*[64]. To achieve iron-limited conditions, 2,2'-dipyridyl or ethylenediamine-*N*,*N*'-diacetic acid (EDDA) was added to *V. parahaemolyticus* (Fig. 2). Only the addition of 2,2'-dipyridyl, but not EDDA, induced a threefold increase of *tdh* fusions. The differential effect of these two iron chelators needs to be defined. Increased *tdh* expression by 2,2'-dipyridyl suggested the presence of transcription factor(s) involved in this iron control of *tdh* expression. In many bacteria, ferric uptake regulator (Fur) and iron-sulfur cluster regulator (IscR) are involved in the iron-associated control of gene expression. Fur protein affects the expression of diverse genes by binding to the Fur boxes[31]. In *Vibrio* species, Fur protein represses the virulence-associated genes including hemolysin and quorum-sensing regulator[64]. IscR is a global regulator controlling the expression of more than 40 genes, including additional proteins involved in Fe-S cluster biogenesis[55]. Deletion mutants of two candidate regulators, *fur* and *iscR*, were constructed and their role in *tdh* expression was examined (Fig. 3 and 4). However, the expression level of the *tdh* gene in the *fur* or *iscR* mutant was not different to the wild-type. These results indicate that Fur and IscR do not mediate iron control of *tdh* expression, and suggest the presence of another regulatory transcription factor(s) of the *tdh* gene under iron-limiting conditions.

Bile is present in the human intestine and facilitates digestion. Bile acids, which are a mixture of the sodium salts of taurocholic, glycocholic, deoxycholic,

chenodeoxycholic, and cholic acid, are a major component of crude bile and are secreted by the gallbladder into the proximal portion of the duodenum to an estimated concentration of 0.2-2% for individual bile acids. They aid in lipid solubilization and also serve to protect the host against enteric pathogens, presumably due to bacteriocidal activity related to their detergent-like properties[50]. To examine the role of bile in *tdh* expression, crude bile or bile salt was added to *V. parahaemolyticus* carrying the *tdh* fusion (Fig. 5). Expression of *tdhA* and *tdhS* by crude bile was induced more than sixfold and ninefold, respectively, though bile salts effected a lower increase in their expression. This data suggest that some molecule(s) included in crude bile, but not bile salt, plays a critical role in *tdh* expression. Therefore, a ligand-fishing experiment was performed to determine the transcription factor(s) that activate *tdhA* expression in the presence of crude bile (Fig. 6). Three proteins bound to the promoter region of *tdhA* compared with the *tdhA* cording region were identified as phage shock protein (psp) operon regulator, a LysR-type transcriptional regulator (LTTR), and a copper-sensing response regulator CusR. In response to extracytoplasmic stresses, the psp system plays multiple roles; i.e., maintaining proton-motive force, protein export by the *sec* and *tat* pathways, survival in stationary phase at alkaline pH, biofilm formation, and virulence in animals[66,67,68]. LTTR is an autoregulatory transcriptional regulator that activates divergent transcription of linked target genes or unlinked regulons encoding extremely diverse functions. It is composed of three or four domains: amino-terminal DNA-binding domain highly conserved helix-turn-helix motif,

coinducer recognition/response domains, carboxyl-terminal domain[69]. The smallest band of 25 kDa was CusR. The *E. coli cusRS* system appears to encode a two-component signal transduction system. Deletion of *cusRS* abolished copper-inducible gene expression, which confers the microorganism with some defense against host responses such as resistance to reactive oxygen species generated by macrophages[70]. However, the role of these transcription factors should be examined via further investigation such as deletion mutagenesis of these corresponding genes.

Numerous effects of crude bile on *V. cholerae* have been described. Provenzano reported that bile increases OmpU expression and transcription in a ToxR-dependent manner in *V. cholerae*. ToxR is a 32-kDa inner-membrane protein, and the *toxR* deletion mutant is defective in the production of CT. John J. Mekalanos et al. report that purified bile acids activate CT expression in a ToxRS-dependent and ToxT-independent manner[40,41,42]. The *toxRS* sequence is present in all strains of *V. parahaemolyticus* regardless of the KP phenotype, and thus, ToxRS is considered a global regulator of *V. parahaemolyticus* genes. Expression of the *tdh* genes was influenced by the products of the *V. parahaemolyticus toxRS* operon cloned from a KP-positive strain; overexpression of the Vp-*toxRS* operon increased expression of the *tdhA* and *tdhS* genes by 1.25- and 5.07-fold, respectively, in an *E. coli* system. In this study, we observed the role of ToxR in bile-induced *tdhA* expression. In the absence of crude bile, *tdhA* expression was barely different between the wild-type and *ΔtoxR* mutant. However, increased activity of the *tdhA::luxAB* fusion with crude bile disappeared in the *ΔtoxR* mutant (Fig. 8). Western blot analysis using the

wild-type or *ΔtoxR* mutant *V. parahaemolyticus* secretome also showed increased protein levels of TdhA by crude bile in the wild-type but not *ΔtoxR* mutant. These results indicate that ToxR plays a role in bile-induced expression of the *tdhA* gene. In an effort to confirm the *ΔtoxR* mutant, expression of a well-known target protein of ToxR, OmpU was also examined. As expected, expression of OmpU was defective in the *ΔtoxR* mutant. Two distinct mechanisms of ToxR-mediated control are known, which occur in a ToxT-dependent manner or via direct binding by ToxR. Because *V. parahaemolyticus* has no *toxT* gene, the regulation of *tdhA* may be achieved via direct binding with ToxR[71]. The cytoplasmic DNA-binding region of *V. parahaemolyticus* ToxR was predicted as the DNA-binding domain, and proved that recombinant cytoplasmic ToxR protein binds to the *tdhA* promoter directly (Fig. 9).

In addition to expression pattern of Tdhs, the action of TdhA was examined using rTdhA and HT-29 cell lines. Previous studies have reported that TdhA has hemolytic activity, cytotoxicity, and enterotoxicity[17,18,19]. Park KS demonstrated that *tdh* deletion mutants showed attenuated mouse lethality. In this study, rTdhA was prepared from secreted proteins derived from *V. parahaemolyticus* grown in the presence of crude bile, and purified using its histidine-tag (Fig. 10). Because gastroenteritis is the main clinical sign of patients infected with *V. parahaemolyticus,* a human gastrointestinal cell line, HT-29, was used. Transmission electron microscopy of rTdhA-treated HT-29 cells showed a dramatic change in morphology (Fig. 11), which includes loss of membrane integrity,

membrane blebbing, appearance of vacuoles, and cell lysis, all of which are hallmarks of necrosis[53]. Both FACS analysis (Fig. 13) and florescence microscopy (Fig. 12) of rTdhA-treated HT-29 cells double-stained with Annexin V and PI clearly indicated that both apoptosis and necrosis are involved in rTdhA-induced cell death. Studies conducted by other groups reported that the TdhA of *V. parahaemolyticus* induced DNA fragmentation, and its cytotoxicity was reduced by ZVAD-FMK, pan-caspase inhibitor, suggesting apoptotic cell death[72,73]. In contrast, TdhA was found to cause colloidal osmotic hemolysis to erythrocytes and Rat-1 cells, which is consistent with necrotic cell death[74]. Diverse phenomena of TdhA-treated cells suggested that cell death caused by *V. parahaemolyticus* may vary according to cell culture conditions, infection time, concentration of TdhA protein, and host cell line types. Therefore, the TdhA of *V. parahaemolyticus* can induce cell death via necrosis and apoptosis. A decrease of cytotoxicity of rTdhA-treated cell by necrostatin-1 also includes necroptosis to pathways involved in rTdhA-mediated cell death.

Chapter II

Role of VcrD1 protein in expression and secretion of flagellar components in *V. parahaemolyticus*

I. INTRODUCTION

Vibrio parahaemolyticus, a common resident in marine and estuarine environments[75], infects humans and typically results in gastroenteritis[76]. In addition to a well-known virulence factor of *V. parahaemolyticus*, thermostable direct hemolysin (Tdh)[17], the type III secretion system (T3SS) is considered to be an important virulence factor for delivering effectors into host cells. Genome sequencing of *V. parahaemolyticus* RIMD2210633 has revealed the presence of two T3SS, T3SS1 and T3SS2. The roles of these T3SSs were examined using T3SS1- or T3SS2-deficient *V. parahaemolyticus* strains, in which the *vcrD1* or *vcrD2* gene, respectively, were mutated. The phenotypes of these mutants indicated that T3SS1 plays a role in cytotoxicity toward tissue culture cells, whereas T3SS2 is associated with bacterial enterotoxicity in the rabbit ileal loop model[8,77]. A T3SS1-deficient *V. parahaemolyticus* strain was also defective in inducing the death of HEp-2 cells, which occurs via a MAPK-dependent (p38 and ERK1/2) and caspase-independent mechanism[78].

In this study, several polar flagellar proteins were secreted at lower levels in the media grown by the *vcrD1* mutant *V. parahaemolyticus* than the culture media of the wild-type strain. The secretion system for bacterial flagellar components belongs to the T3SS superfamily[79]. While the T3SSs responsible for secreting effectors are defined as non-flagellar (NF) T3SSs, they are thought to have evolved from flagellar T3SSs[80]. *V. parahaemolyticus* has two flagellar systems, i.e., a polar

sheathed flagellum and lateral unsheathed flagellar[81,82]. The polar flagellum functions constitutively and is responsible for bacterial swimming. On the other hand, synthesis of a lateral flagellar is induced under a specific condition such as growth on solid surfaces[83].

Approximately 60 genes are involved in the formation of the polar flagellum in *V. parahaemolyticus*[84]. Most of the polar flagellar genes are found in two locations of the larger chromosome of *V. parahaemolyticus* with the exceptions of several motor genes, *motAB*, *motX*, and *motY*[85]. Transcription of these flagellar genes is temporally regulated in tight coordination with the orders of flagellar assembly[84]. These flagellar genes are grouped into three hierarchies according to their temporal orders of transcription during flagellar formation. The early genes, *flaK* and *flaLM*, are master regulators that interact with σ54 and play a role in transcription of the middle genes. Interestingly, the *flaK* mutant *V. parahaemolyticus* was found to retain the swimming motility until the bacteria had an additional defect in formation of the lateral flagellar, indicating the presence of cross-regulation between these two flagellar systems of *V. parahaemolyticus*[92]. The middle flagellar genes transcribed by σ54 encode proteins involved in assembly of the hook-basal-body structure, HAP1, HAP3, MotY, some chemotaxis proteins, and an alternative sigma factor, σ28. Sigma factor 28 then transcribes the other set of flagellar genes, the late flagellar genes, which encode additional motor proteins, additional chemotaxis proteins, five flagellins, a distal capping protein HAP2, and the anti-σ28 FlgM.

Besides flagellar T3SSs, *V. parahaemolyticus* possesses two NF T3SSs (T3SS1 and T3SS2) to convey its virulence factors into the host cells[8,84]. In this study, we further characterized the role of NF-T3SS1 in polar flagellar formation by examining the altered expression and secretion of flagellar components in a *ΔvcrD1* mutant.

II. MATERIALS AND METHODS

1. Bacterial strains, plasmids, and culture conditions

The bacterial strains and plasmids used in this study are listed in Table 3. *Escherichia coli* strains used to prepare plasmid DNA and transfer of the plasmid by conjugation were grown in Luria-Bertani (LB) broth (1% bacto-tryptone, 0.5% yeast extract, and 1% NaCl) or on LB plates containing 2% agar. *V. parahaemolyticus* RIMD2210633 (ATCCBAA-238; American Type Culture Collection, Mannassas, VA) was used as the wild-type strain in this study and was cultured in LB medium supplemented with an additional 3% NaCl (LBS). Ampicillin was added to the medium at 100 μg/ml to maintain the plasmids in *E. coli*. Chloramphenicol (2 μg/ml) was used to select *V. parahaemolyticus* exconjugants. All medium components were purchased from Difco (Lawrence, KS, USA), and the chemicals and antibiotics were sourced from Sigma (St. Louis, MO, USA).

2. Preparation of secreted proteins from *V. parahaemolyticus*

Secreted proteins were prepared from wild-type and *ΔvcrD1 V. parahaemolyticus* strains cultivated in LBS broth at 37°C. Once bacterial cells grew to an optical density at 600 nm (OD_{600}) of 0.8, they were centrifuged at 8,000 rpm for 15 min at

4°C, and the resultant supernatants were passed through a 0.2-μm pore membrane filter. Proteins were concentrated using a Centricon YM-10 (Millipore, Bedford, MA) at 4°C. Filtered supernatants were mixed with an equal volume of prechilled 10% TCA and incubated on ice for 30 min. After a 30-min centrifugation at 9,000 rpm and 4°C, the pellets were washed with acetone three times, dried, and resuspended in lysis buffer (50 mM NaH_2PO_4, 300 mM NaCl, and 10 mM imidazole, pH 8.0). The protein content in the secretome preparations was determined with a protein assay kit (Bio-Rad, Hercules, California).

3. Preparation of polyclonal antibodies

The DNA encompassing the ORF of each selected protein (FlgL, FlgM, and OmpV) was amplified using a pair of specific primers listed in Table 4 and cloned into a pET21b (+) expression vector (Novagen, Darmstadt, Germany) as listed in Table 3. The recombinant candidate protein was overexpressed by adding 1 mM isopropyl thio-β-D-galactoside (IPTG), and then separated by 12% SDS-PAGE. The induced protein band was excised, and resuspended with phosphate-buffered saline (PBS: 137 mM NaCl, 2.7 mM KCl, 10 mM Na_2HPO_4, and 2 mM KH_2PO_4, pH 7.4). This protein was then injected intraperitoneally into pathogen-free rats (CrjBgi: CD[S.D.]IGS, 6-week-old, female) as an antigen to produce polyclonal antibodies. After three injections at two-week intervals, serum was obtained from the immunized rats, and the resultant antibody titers were tested.

4. Western blot analysis

Bacterial extracts were prepared by sonicating bacterial cells in TNT buffer (10 mM Tris-HCl, pH 8.0, 150 mM NaCl, and 0.05% Tween 20). Protein in the culture supernatants was concentrated 200-fold by precipitation with trichloroacetic acid (TCA) or by filtration through Amicon/Centricon YM-10 columns (Millipore, Billerica, MA). Cell lysates and concentrated supernatants in sample buffer (50 mM Tris-HCl, pH 6.8, 100 mM dithiothreitol, 2% SDS, 0.1% bromophenol blue, and 20% glycerol) were separated by SDS-PAGE and transferred to polyvinylidene fluoride (PVDF) membranes (Millipore). Membranes were blocked with 5% skim milk in Tris-buffered saline with Tween 20 (TBST; 150 mM NaCl, 50 mM Tris-HCl, and 0.1% Tween 20) and incubated overnight at 4^{o}C with polyclonal antibodies (1:5,000 dilution). Horseradish peroxidase (HRP)-conjugated secondary antibodies were used. Immuno-reactive bands were visualized using an enhanced chemiluminescence system (Amersham, Buckinghamshire, United Kingdom).

In addition to antibodies against candidate proteins, secretion of FlgE and FlaA was monitored using antibodies specific to homologous proteins from *V. vulnificus* (Lee et al. 2003; K.-H. Lee and J. A. Kim unpublished result, respectively). Antibodies specific to Tdh[78] were included in the Western blot analyses as a loading control for each secretome.

5. Construction of deletion mutants of *V. parahaemolyticus*

A. *Δ exsA* and *ΔexsAΔvcrD1* mutants

For construction of the *ΔexsA* mutant, the downstream region of the *exsA* gene was amplified from the genomic DNA of *V. parahaemolyticus* RIMD2210633 with the primers, exsA-downF and exsA-downR (Table 4). The resultant 792-bp DNA fragment was then digested with *S*alI and *S*acI, and ligated into pBlueScript (II) SK (+) to produce pSKexsAD. The upstream region of the *exsA* gene was amplified using the primers, exsA-upF and exsA-upR (Table 4). The resultant DNA fragment of 747 bp was treated with *A*paI and *X*baI and ligated into pSKexsAD to yield pSKexsAUD. The 1,539-bp *A*paI-*S*acI DNA fragment of pSKexsAUD was transferred into a suicide vector pDM4[45], resulting in formation of pDM4exsAUD. The plasmid pDM4exsAUD in SM10 λ*pir* [48] was mobilized to *V. parahaemolyticus* RIMD2210633 or the *ΔvcrD1* mutant, and the conjugants were selected by plating the conjugation mixture of *E. coli* and *V. parahaemolyticus* on LBS plates supplemented with 2 μg/ml chloramphenicol. A colony with characteristics indicating a double homologous recombination event (resistance to 5% sucrose and sensitivity to chloramphenicol) was further confirmed by PCR using the primers, exsA-upF and exsA-downR, and then named MJ21 or MJ22 for the *ΔexsA* or *ΔexsAΔvcrD1* mutant strain, respectively.

B. *ΔflaKΔlafK* mutant

A mutant *V. parahaemolyticus* missing both FlaK and LafK, key regulators for the polar flagellum and lateral flagellar, respectively[92], was constructed and included for motility assays as a non-motile control. For construction of the *ΔflaK* mutant, the upstream (766-bp) and downstream (647-bp) regions of the *flaK* gene were amplified using the primer set of flaK-upF/flaK-upR and flaK-downF/flaK-downR, respectively (Table 4). The *X*hoI-*S*peI DNA fragment of pSKflaKUD was transferred into pDM4 for replication in pDM4flaKUD, which was then used to generate the *ΔflaK* mutant, as described above. A plasmid (pSKlafKUD), including the upstream (750-bp) and downstream (640-bp) regions of the *lafK* gene, was amplified by the following primer sets, lafK-upF/lafK-upR and lafK-downF/lafK-downR (Table 4). The *A*paI-*S*acI DNA fragment of the resultant plasmid was ligated into pDM4 to produce pDM4lafKUD, which was used to make the *ΔflaKΔlafK* mutant, as described above.

6. Motility assay

Wild-type and mutant *V. parahaemolyticus* strains *(ΔvcrD1*, *ΔexsA*, *ΔexsAΔvcrD1*, and *ΔflaKΔlafK* mutants) were freshly grown in LBS at 37^{o}C with aeration to an OD_{600} of 0.8, washed, and resuspended in PBS to a final concentration of 10^6 CFU/ml. The cell suspension was inoculated into LBS medium containing 0.3%

agar and incubated for 4 hrs at 37°C. Motility of the *vcrD1* mutant *V. parahaemolyticus* carrying the complementation plasmid, pRKvcrD1[78], was also examined in the same manner along with two control strains (wild-type carrying pRK415 and *vcrD1* mutant carrying pRK415).

7. Transmission electron microscopy

The *vcrD1* knockout mutant was examined for the presence of a flagellum. Bacterial cells were negatively stained with 2% (wt/vol) uranyl acetate (pH 7.4) on a Formvar carbon-coated grid and observed with a transmission electron microscope (CM-10; Philips) at 75 kV.

8. Fractionation of bacterial cells

Wild-type and *ΔvcrD1 V. parahaemolyticus* strains were grown to OD_{600}= 0.8 at 37°C in LBS broth. Through centrifugation, the culture supernatant was separated from the bacterial cells. The harvested cells were divided into cytoplasmic and periplasmic fractions as described by Manoil and Beckwith[86]. Harvested cells were resuspended in a spheroplast buffer (100 mM Tris-HCl, pH 8.0, 0.5 mM EDTA, 0.5 mM sucrose, 1 mM $MgCl_2$, and 20 μg/ml phenylmethylsulfonyl fluoride), and subjected to centrifugation (3 min, 13,000 rpm, 4℃). The pellets were warmed,

resuspended in ice-cold water, and treated with 20 mM $MgCl_2$. The osmotically shocked cells were centrifuged (5 min, 13,000 rpm, 4℃). The supernatants were saved as periplasmic fractions, and the pellets were further resuspended in PBS with 1% Triton X-100. The cells in the pellet were lysed by sonication. After centrifugation, the resultant supernatant was saved as the cytoplasmic fraction. The culture supernatant, periplasmic fraction, membrane fraction, and cytoplasmic extract for each strain were analyzed by Western blot using anti-FlaA antibodies or anti-FlgM antibodies. Antibodies against glucose-specific enzyme IIAGlc (Lee et al. unpublished result) and anti-OmpV antibodies were used as a loading control for cytoplasmic and membrane fractions, respectively. An anti-Tdh antibody was used as a loading control for the secretome.

9. Quantitation of flagellar mRNAs

The degree of expression of seven flagellar mRNAs was evaluated in wild-type and *ΔvcrD1* mutant *V. parahaemolyticus* by real-time PCR. The wild-type and *ΔvcrD1* mutant *V. parahaemolyticus* were cultured in LBS broth at 37°C with shaking. At OD_{600}= 0.8, the bacteria cells were centrifuged at 8000 rpm for 5 min at 4°C. Total RNAs were isolated from harvested wild-type or *ΔvcrD1* mutant *V. parahaemolyticus* strains using TRizol (BioRad) and treated with the RNase-free DNase (Qiagen). After the amount of RNA was measured using NanoDrop ND-1000 (Thermo Fisher Scientific, Wilmington, USA), cDNA was synthesized from 4

μg of RNA using the PrimeScript RT reagent kit (TaKaRa, Shiga, Japan) following the manufacturer's directions. cDNA was analyzed by quantitative real-time PCR (qRT-PCR) on a Light Cycler 480 II real-time PCR system (Roche Applied Science, Mannheim, Germany) using Light Cycler 480 DNA SYBR green I master kit (Roche Applied Science). The qRT-PCR was carried out in a 96-well plate. The amount of each gene mRNA estimated using the specific pairs of primers is shown in Table 4. The experiments were performed in triplicate for each sample and results were measured along with the standard deviation. The gene encoding glyceraldehyde-3-phosphate dehydrogenase (*gap*) of *V. parahaemolyticus* was used as an endogenous normalized control for each reaction gene in the wild-type and *ΔvcrD1* mutant cDNA. The quantification analysis was carried out using the crossing point (Cp) of the Light Cycler 480 II real-time PCR system software program (Roche Applied Science, version LSC480 1.5.0.39).

10. Statistical analysis

Data are presented as the means ± standard deviation from three independent experiments. Statistical analyses were performed using the student's t test (SYSTAT, SigmaPlot version 11; Systat Software Inc. Chicago, IL) to evaluate the statistical significance of the results. Differences were considered significant when $P < 0.05$. Data with $P < 0.01$ are indicated with two asterisks(**), whereas data with P-values between 0.01 and 0.05 are indicated with a single asterisk(*).

Table 3. Bacterial strains and plasmids used in this study

Strains /plasmids	Description	Source /reference
E. coli		
DH5α	*supE44, ΔlacU169* (Φ80 *lacZ ΔM15*), *hsdR17, recA1, endA1, gyrA96, thi-1, relA1*	Invitrogen
SM10 λ*pir*	*thi thr leu tonA lacy supE recA*::RP4-2-Tc::Mu λ*pir*, OriT of RP4 Km^r; conjugational donor	48
BL21 (DE3)	*E. coli* B F^- *dcm ompT hsdS* (rB^- mB^-) *gal* λ (DE3)	Invitrogen
Vibrio parahaemolyticus		
RIMD2210633	KP positive, serotype O3:K6	ATCC
NK1	*ΔvcrD1* mutant derived from RIMD2210633	78
MJ21	*ΔexsA* mutant derived from RIMD2210633	This study
MJ22	*ΔexsA* mutant derived from NK1	This study
MJ23	*ΔflaK* mutant derived from RIMD2210633	This study
MJ24	*ΔlafK* mutant derived from RIMD2210633	This study
MJ25	*ΔlafK* mutant derived from MJ23	This study
Plasmids		
pET21b	Expression vector, Ap^r	Novagen
pET-ompV	pET21b containing 754-bp *ompV*	This study
pET-flgL	pET21b containing 1,191-bp *flgL*	This study
pET-flgM	pET21b containing 315-bp *flgM*	This study
pBluescript SK II (+)	Cloning vector ; *ori*, *oriF1*, *lacZ*; Ap^r	Stratagene

pSKexsAD	pBluescript SK II (+), 792-bp downstream region of *exsA*	This study
pSKexsAUD	pSKexsAD, 747-bp upstream region of *exsA*	This study
pSKflaKU	pBluescript SK II (+), 766-bp upstream region of *flaK*	This study
pSKflaKUD	pSKflaKU, 647-bp downstream region of *flaK*	This study
pSKlafKU	pBluescript SK II (+), 750-bp upstream region of *lafK*	This study
pSKlafKUD	pSKlafKU, 640-bp downstream region of *lafK*	This study
pDM4	Suicide vector; Cm^r	45
pDM4-ΔexsA	pDM4 containing *A*paI-*S*acI fragment of pSKexsAUD	This study
pDM4-ΔflaK	pDM4 containing *X*hoI-*S*peI fragment of pSKflaKUD	This study
pDM4-ΔlafK	pDM4 containing *A*paI-*S*acI fragment of pSKlafKUD	This study
pRK415	Broad-host-range plasmid, Tc^r	47
pRKvcrD1	pRK415 containing 1,035-bp vcrD1	48

∗Ap^r, ampicillin resistance; Cm^r, chloramphenicol resistance; Tc^r, tetracycline resistance

Table 4. Primers used in this study

Primer name	Nucleotide sequence (5'-3')	Enzyme site
For recombinant proteins		
ompV-F	GATCGGATCCGATGAACAAGACACTTATCG	*B*amHI
ompV-R	GATCCTCGAGGGAAGTGGTAAGACACGCTT	*X*hoI
flgL-F	GATCGGATCCGGTGTTAACCCGAATTTCTAG	*B*amHI
flgL-R	GATCCTCGAGAATGTAGTTAAACAATGTCAG	*X*hoI
flgM-F	ATGCGAATTCCATGGCAGGTATAGATAATATA	*E*coRI
flgM-R	ATGCCTCGAGGCTTTTGCCTTGCAATTCGTT	*X*hoI
Construction of mutant strains		
exsA-upF	ATGCGGGCCCAGTGATAGGGAAACTCTATTC	*A*paI
exsA-upR	ATGCCTGCAGTTTCTACCCTTCATAATTTTT	*P*stI
exsA-downF	ATGCCTGCAGAATGACTTATGACTAAAATTT	*P*stI
exsA-downR	ATGCGAGCTCGTGTATTTAGCTGCGCTTTTA	*S*acI
flaK-upF	GATCCTCGAGTCACAAATTCCGTTATGGCCA	*X*hoI
flaK-upR	GATCCTGCAGAAGTAAGAATGATTGCCTTTA	*P*stI
flaK-downF	GATCCTGCAGATCGAGCTTCAGTTCAATCAC	*P*stI
flaK-downR	GATCACTAGTTCGTCGCTGGCGGAAAATTAG	*S*peI
lafK-upF	ATGCGGGCCCGGAACCAAATAATAAGATTTC	*A*paI

lafK-upR	ATGCCTGCAGTGAACCTTAACCTTCTTCTGT	*P*stI
lafK-downF	ATGCCTGCAGCCTAATAGGAGAAAAATATAG	*P*stI
lafK-downR	ATGCGAGCTCCAATCTCGCCAATATCGAATC	*S*acI

For real-time PCR

FlaK-F	AAGCGTTACCACCAGAAGGGG
FlaK-R	CTAACGCTGCAAATTATACTT
FlaL-F	GCCAAAATTATGGAGCCATTTTTT
FlaL-R	TTATTGCGCTTCTGATTGCAC
flgE-F	TGGGGTGAATCAAACAAAGGC
flgE-R	TTATCTAATCTGCAGGATATT
fliF-F	GAAACCAGCCTAATTGGTAGC
fliF-R	TTAGCCATTTTCGTTCATCCA
fliD-F	ATTCGTACGCGAGAGAAAAGT
fliD-R	TTAACCTAACGCACTCATAAG
flaA-F	ATCAGCAACCTAGACAACATA
flaA-R	TTAGCCCAACAAGCTTAGCGC
flgM-F	AGCCAACAAAGTAAAGCCGTC
flgM-R	TTAGCTTTTGCCTTGCAATTC
gap-F	TTTGAAGAGCGTCCGTTGGTG
gap-R	TTAAGCCAACACAACGTTACG

*Restriction enzyme sites are underlined.

Table 5. Proteins secreted less by the *ΔvcrD1* mutant strain of *V. parahaemolyticus*

Spot	Protein (ORF#)	MW (kDa)	pI	Score (valid score)
1	Polar flagellar hook-length control protein FliK (VP2244)	68	4.5	126 (77)
2	Flagellar capping protein (VP2256)	73	4.7	125 (58)
3	Flagellar hook-associated protein FlgK (VP0785)	71	5.5	274 (58)
4	Polar flagellin FlaA (VP2258)	40	4.9	86 (58)
5	Flagellar hook-associated protein FlgL (VP0786)	45	5.5	201 (58)
6	Flagellin (VP0790)	40	4.9	61 (58)
7	Flagellar basal body rod modification protein (VP0777)	25	4.8	132 (58)
8	Flagellar protein FlaG (VP2257)	16	4.7	115 (58)
9	Chitodextrinase (VPA0832)	112	4.6	92 (58)
10	Chitinase (VPA0055)	90	4.4	102 (58)
11	Putative chitinase (VP0619)	63	4.6	48 (58)
12	Alkaline serine protease (VPA0227)	72	4.8	56 (58)
13	Outer membrane protein OmpA (VPA1186)	36	4.6	122 (58)

14	Putative outer membrane protein OmpV (VPA0318)	28	5.1	60 (58)
15	Hypothetical protein (VPA0917)	41	4.8	115 (58)
16	Hypothetical protein (VPA1077)	43	4.3	84 (58)
17	Hypothetical protein (VPA0242)	20	4.8	84 (58)
18	Hypothetical protein (VPA0934)	23	5.6	52 (58)
19	Hypothetical protein (VPA0669)	11	5.9	46 (58)

III. RESULTS

1. Confirmation of down-secreted flagellar proteins in the *ΔvcrD1* mutant by Western blot

To identify the proteins secreted via the T3SS1 apparatus, 2D-gel electrophoresis was performed with bacterial culture supernatants of the wild-type and the *ΔvcrD1* mutant *V. parahaemolyticus* strains, and their proteomic patterns were compared[87]. Among proteins that were present at lower levels in the mutant supernatant, 19 protein spots were identified and are listed in Table 5. A majority of the down-secreted proteins in the *ΔvcrD1* mutant were associated with parts of the polar flagellum: FliK, FlaH, FlgK, and FlgL, which are in the flagellar hook; FlgD, which is a cap protein of a flagellar hook; and FlaA, FlaD, and FlaG, which are flagellins. This result suggests that VcrD1 plays a significant role in the assembly and development of the polar flagella of *V. parahaemolyticus*. Earlier studies reported that T3SS is evolutionarily related to the secretion system for bacterial flagella and flagellar T3SS through sharing of structural and functional features[88]. The other down-secreted proteins are enzymes, including a chitodextrinase, chitinases, and an alkaline serine protease. Two outermembrane proteins, OmpA and OmpV, were also secreted at lower levels in the *ΔvcrD1* mutant. Finally, six hypothetical proteins without any known function were down-secreted, and these proteins were not evaluated in this study.

Two of the eight flagellar proteins identified by 2D gel electrophoresis (Table 5), FlaA and FlgL, were confirmed to exist at low concentrations in the secretome of the *ΔvcrD1* mutant using their specific polyclonal antibodies. A 40-kDa immunoreactive band was present at a lower level in the secretome of the *vcrD1* mutant than in the wild-type (Fig. 15A). When wild-type and *ΔvcrD1* mutant secretomes were analyzed, the *ΔvcrD1* mutant secretome contained less FlgL than did the wild-type secretome (Fig. 15B). We also examined secretion of an additional flagellar protein, FlgE, in the culture supernatants of wild-type and the *ΔvcrD1* mutant by Western blot using antibodies against *V. vulnficus* FlgE[89] (Fig. 15C). Similar to FlaA and FlgL, the *vcrD1* mutant secreted less FlgE than did the wild-type. Concomitant down-secretion of three flagellar proteins suggests that overall expression of flagellar proteins is decreased in the *ΔvcrD1* mutant. Therefore, polyclonal antibodies were made against recombinant FlgM of *V. parahaemolyticus*, an anti-sigma factor that controls the temporal expression of flagellar genes, especially late genes[90]. Western blot analysis of culture supernatants demonstrated that less FlgM was present in the culture supernatant of the *ΔvcrD1* mutant (Fig. 15D). The Tdh levels in wild-type and *vcrD1* mutant secretomes were evaluated by Western blot with anti-Tdh antibodies as a loading control.

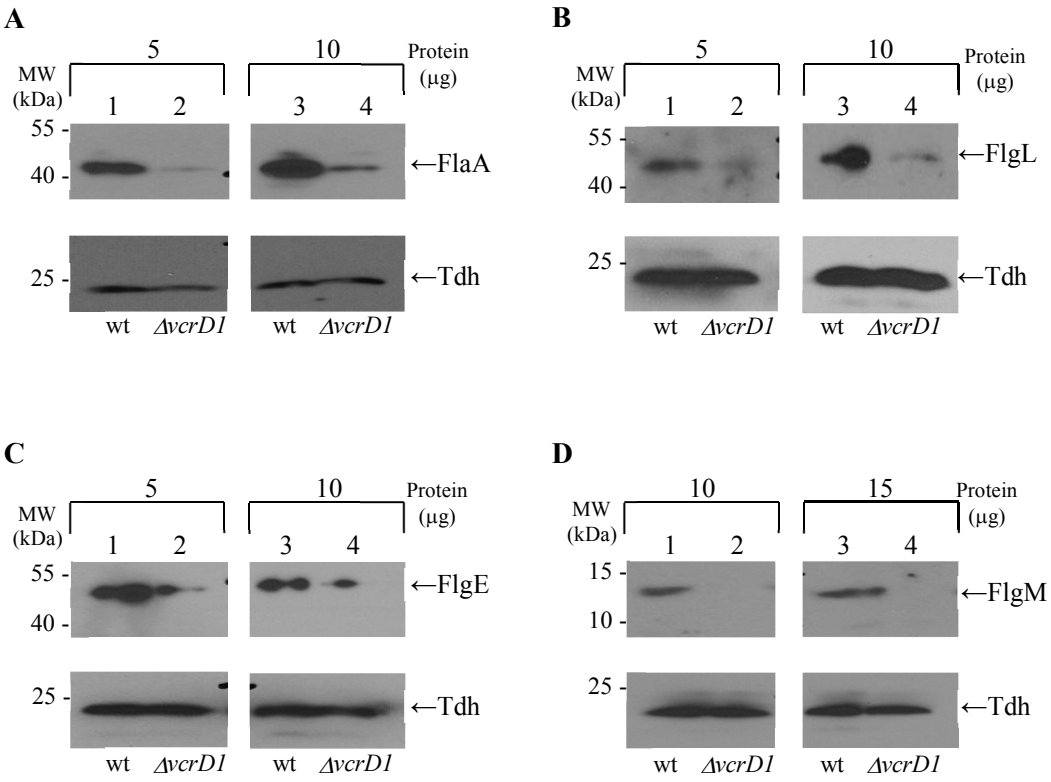

Figure 15. Western blot analysis of secretomes of wild-type and *ΔvcrD1* mutant strains using polyclonal antibodies against four selected flagellar proteins. A- Western blot using anti-FlaA antibodies, B- anti-FlgL antibodies, C- anti-FlgE antibodies, D- anti-FlgM antibodies, and anti-Tdh antibodies (as a loading control). Lanes 1, 3; secretomes of wild-type, lanes 2, 4; *ΔvcrD1* secretomes.

2. Role of *vcrD1* in bacterial flagella/motility of *V. parahaemolyticus*

Spotting the bacterial suspensions on LBS medium containing 0.3% agar showed that the *ΔvcrD1* mutant strain did not have any motility and appeared as a small and sharply delineated cell mass, whereas wild-type *V. parahaemolyticus* had a distinct motile phenotype with a large diffuse spreading halo (Fig. 16A). Transmission electron microscopy clearly showed that wild-type *V. parahaemolyticus* retained a polar flagellum, but that the *ΔvcrD1* mutant had completely lost its flagellum (Fig. 16B). To confirm that loss of bacterial motility in the *ΔvcrD1* is derived from absence of the *vcrD1* gene, a complementation strain, a *ΔvcrD1* mutant carrying pRKvcrD1, was examined for its motility along with two control strains, wild-type with pRK415, *ΔvcrD1* with pRKvcrD1 or pRK415 (Fig. 16C). As expected, wild-type *V. parahaemolyticus* with pRK415 had motility, whereas the *ΔvcrD1* mutant carrying pRK415 did not show any motility. The *ΔvcrD1* mutant with pRKvcrD1 had motility comparable with wild-type with pRK415.

A

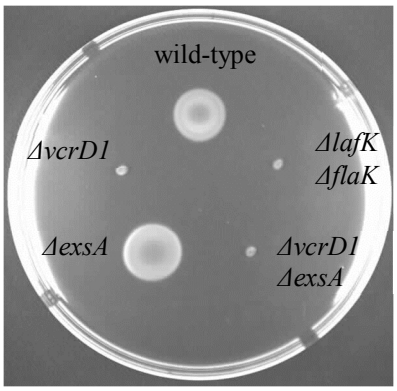

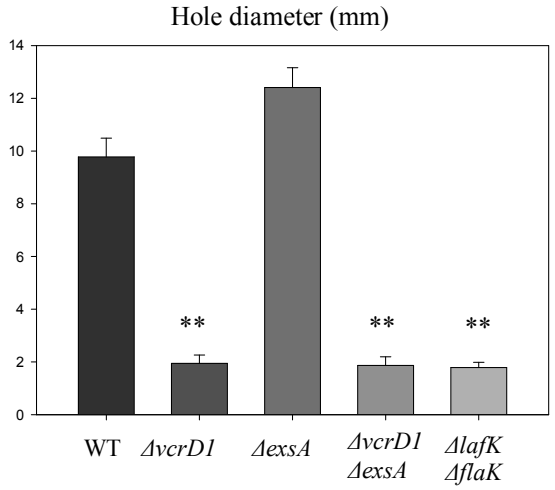

B

Wild-type

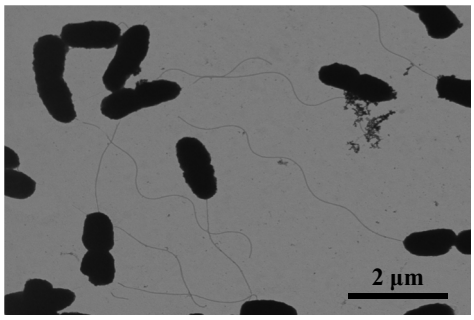

ΔvcrD1

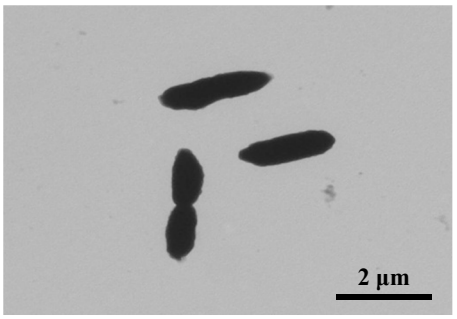

C

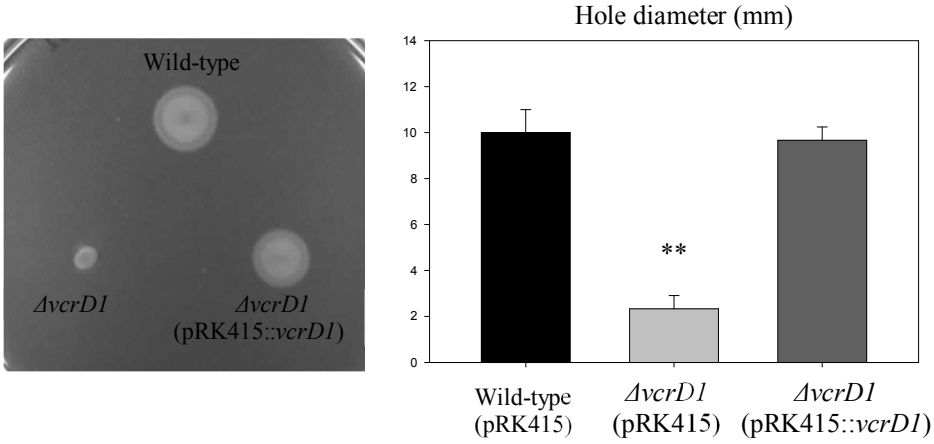

Figure 16. Bacterial motility and polar flagellum of wild-type and *ΔvcrD1* mutant strains of *V. parahaemolyticus*. A- Swimming motility of *V. parahaemolyticus* strains on 0.3% agar plates. A mutant *V. parahaemolyticus* missing FlaK, LafK, and ExsA key regulators for polar flagellum, lateral flagella, and T3SS, respectively, was used as a control. B- Transmission electron micrographs of wild-type and *ΔvcrD1* mutant strains negatively stained with uranyl acetate. The bar represents 2 μm. C- Swimming motility of wild-type carrying pRK415, *ΔvcrD1* mutant strain carrying pRK415, and *ΔvcrD1* mutant strain carrying pRKvcrD1 on 0.3% agar plates.

3. Determination of the expression level of flagellar components in wild-type and *ΔvcrD1* mutant *V. parahaemolyticus* strains

Since four flagellar proteins were present at lower levels in the culture supernatant of the *ΔvcrD1* mutant, we examined the cellular fractions containing these proteins in the *ΔvcrD1* mutant *V. parahaemolyticus*. Specifically, we determined whether FlaA or FlgM in the cytoplasm of the *ΔvcrD1* mutant was not successfully secreted through the outer membrane. Extracts of wild-type and *ΔvcrD1 V. parahaemolyticus* strains were divided into four fractions (cytoplasmic, periplasmic, membrane, and culture supernatant) that were analyzed by Western blot using anti-FlaA or anti-FlgM antibodies (Fig. 17A and 17B, respectively). FlaA was detected in all four fractions from the wild-type strain, but was barely detected in any fraction from the *ΔvcrD1* strain, indicating that decreased secretion of FlaA in the mutant resulted from decreased FlaA synthesis. FlgM was mainly found in the cytoplasm and secretome of wild-type cells. The amount of FlgM in all four fractions from the *ΔvcrD1* mutant decreased. The levels of both FlgM and FlaA decreased in all the fractions of the *ΔvcrD1* mutant, raising a possibility that transcription of flagellar genes is down-regulated in the T3SS1-defective mutant.

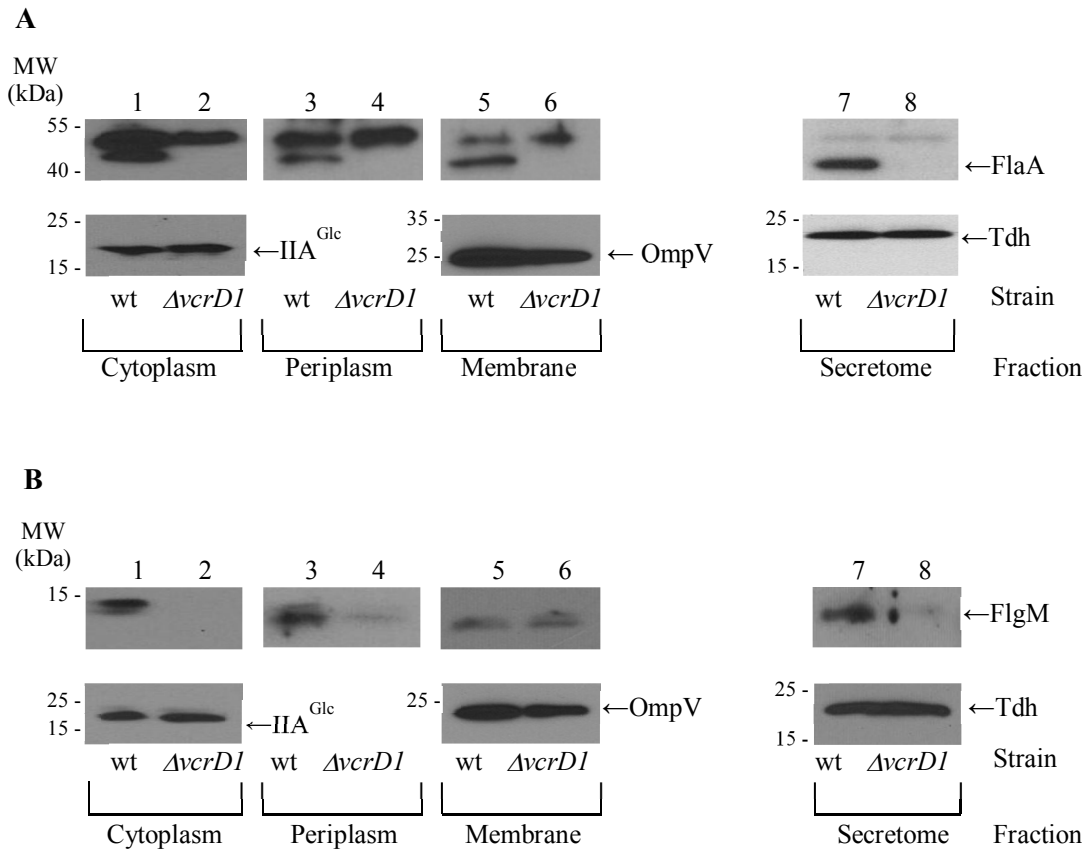
A
MW
(kDa)
1 2 3 4 5 6 7 8
55 -
40 -
25 -
15 -
35 -
25 -
←FlaA
←Tdh
←IIA Glc
← OmpV
wt ΔvcrD1 wt ΔvcrD1 wt ΔvcrD1 wt ΔvcrD1 Strain
Cytoplasm Periplasm Membrane Secretome Fraction
B
MW
(kDa)
1 2 3 4 5 6 7 8
15 -
25 -
15 -
←FlgM
←IIA Glc
←OmpV
←Tdh
wt ΔvcrD1 wt ΔvcrD1 wt ΔvcrD1 wt ΔvcrD1 Strain
Cytoplasm Periplasm Membrane Secretome Fraction

Figure 17. Fractionation of wild-type and *ΔvcrD1* mutant *V. parahaemolyticus* into cytoplasmic, periplasmic, membrane, and secretome proteins and Western blot analysis of these fractions using anti-FlaA antibodies (A) or anti-FlgM antibodies (B). Lanes 1, 3, 5, and 7, cytoplasmic, periplasm, membrane, and secretome proteins of wild-type *V. parahaemolyticus*, respectively; lanes 2, 4, 6, and 8, cytoplasmic, periplasm, membrane, and secretome proteins of *ΔvcrD1 V. parahaemolyticus*, respectively. Intracellular level of glucose-specific enzyme IIA^{Glc} was monitored as a control for cytoplasmic protein, whereas OmpV serves as a loading control for membrane proteins. Tdh is a loading control for secretome proteins.

4. Determination of transcription level of flagellar genes in wild-type and *ΔvcrD1* mutant *V. parahaemolyticus*

Using primers designed to amplify specific flagellar genes (Table 4), the levels of flagellar gene transcripts were monitored in the wild-type and *ΔvcrD1* mutant strains (Fig. 18). The *gap* gene encoding glyceraldehyde-3-phosphate dehydrogenase was constitutively expressed. Therefore, all transcript levels were normalized to the amount of *gap* transcript in the same RNA sample. Expression of two early flagellar genes, *flaK* and *flaL*, was not affected in the *ΔvcrD1* mutant. Transcripts of the middle (*flgE*, and *fliF*) and late (*fliD*, and *flaA*) flagellar genes were decreased significantly in the *ΔvcrD1* mutant (from 28% to 3% of wild-type). In addition, expression of the *flgM* gene was also reduced in the *ΔvcrD1* mutant, which is an anti-σ factor and one of the middle/late genes. This result demonstrated that deficiency of *vcrD1* resulted in decreased transcription of flagellar genes, especially middle and late flagellar genes.

.

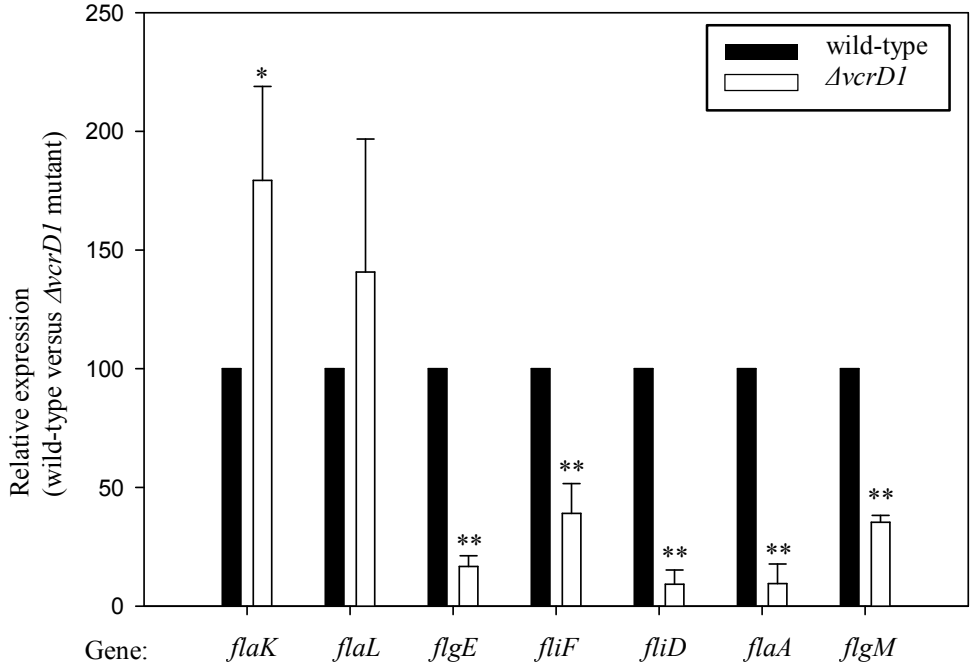

Figure 18. Quantitative analysis of transcripts of seven flagellar genes. Total RNAs were isolated from wild-type or *ΔvcrD1* mutant *V. parahaemolyticus* strains and treated with RNase-free DNase. After being converted into cDNAs using the PrimeScript RT reagent kit, transcript levels were analyzed by reverse transcriptase-PCR (RT-PCR) on a Light Cycler 480 II Real-Time PCR system (Roche Applied Science) with Light Cycler 490 DNA SYBR Green I master. RT-PCR was carried out in triplicate in a 96-well plate using the primers shown in Table 4. The gene encoding NAD-dependent glyceraldehyde-3-phosphatase (*gap*) of *V. parahaemolyticus* was used as an endogenous loading control for the reactions. These results were quantified by the Light Cycler 480 II Real-Time PCR system software program.

IV. DISCUSSION

Two kinds of T3SSs in *V. parahaemolyticus* have been implicated in the delivery of effector proteins to the host cell cytoplasm[8]. Both kinds are NF-T3SSs. Knocking out the conserved inner membrane proteins, VcrD1 or VcrD2[91], decreased the cytotoxicity and enterotoxicity, respectively[8,78]. VcrD1 is postulated to be a conserved member of the NF-T3SS secretion apparatus[91]. *V. parahaemolyticus* has a dual flagellar system: 1) a single polar flagellum that is continuously produced and 2) numerous lateral flagella that are synthesized under certain conditions, such as surface conditions[81]. The transcriptional cascade for the *V. parahaemolyticus* polar flagellum has been analyzed[84], and LafK, a regulator for lateral flagellar genes, also plays a role in morphogenesis of the polar flagellum[92]. Further characterization of the *ΔvcrD1* mutant *V. parahaemolyticus* showed decreased secretion of several flagellar components (Table 5, and Fig. 15) and raised the possibility that VcrD1, a component of NF T3SS1, also plays a role in assembling the polar flagellum.

As expected, the *ΔvcrD1* mutant had no bacterial motility or polar flagellum (Fig. 16). The absence of a polar flagellum in the *ΔvcrD1* mutant of *V. parahaemolyticus* indicates that the VcrD1-containing T3SS system might function in flagellum secretion. *V parahaemolyticus* has 60 potential flagellar genes, and their roles in flagellum assembly and transcriptional organization have been reported[84]. Therefore, further experiments are needed to reveal how VcrD1 is

involved in flagellum formation. For example, physical association of VcrD1 with other flagellar components should be a focus of future research.

The lower cytoplasmic level of FlaA protein in the *ΔvcrD1* mutant suggests that decreased FlaA secretion could be caused by decreased expression of FlaA (Fig. 17A). Flagellum morphogenesis is a complex cascade of events that requires coordinated expression of more than 60 genes encoding structural subunits, regulatory proteins, and chemo-sensor machinery. These genes have been categorized into three groups in relation to their temporal expression during assembly of the polar flagellum: early, middle, and late genes[93].

Early genes encode FlaK and FlaLM, transcriptional regulators required for expression of the middle genes. The middle genes transcribed by σ54 include ORFs encoding assembly proteins, σ28, hook proteins, and basal body proteins. Sigma 54 also transcribes the late genes encoding flagellins, motor proteins, and the anti-σ factor, FlgM[85]. FlgM is an important regulatory factor for temporal coordination of flagellar gene expression, which blocks premature expression of late filament genes by binding to FliA. Secretion of FlgM through a complete hook basal body results in expression of the late filament genes[94]. Therefore, we examined whether decreased expression of flagellar proteins is caused by the altered level of cytoplasmic FlgM (Fig. 17B). Western blot analysis of cytoplasmic fractions and secretomes indicated that FlgM expression is also decreased in the *ΔvcrD1* mutant *V. parahaemolyticus*. This result suggests that the altered FlaA level is not due to

increased cytoplasmic FlgM resulting from failed FlgM secretion.

Quantitative measurement of flagellar transcripts demonstrated that the *ΔvcrD1* mutation affected early genes and middle/late genes differently (Fig. 18). Failed secretion of flagellar components has been reported to result in abortion of transcription of downstream flagellar genes[95]. Malfunctioning flagellar secretion caused by VcrD1 deficiency does not interfere with the early steps of flagellum assembly, but prevents the transcriptional cascade in the middle and late stages of flagellum morphogenesis.

This observation suggests that the role of T3SS1 in cytotoxicity of *V. parahaemolyticus* should be re-evaluated. The loss of polar flagellum/motility in the *ΔvcrD1* mutant (Fig. 16) may be a factor responsible for the attenuated cytotoxicity of the mutant. In *V. vulnificus*, flagellum/motility has been reported as an important virulence factor[46]. So far, three effector proteins delivered by T3SS1 have been identified: VopQ (VepA)[96], VopS[97], and VPA0450[98]. To define the exact role of T3SS1 as an NF-T3SS, additional mutants that are defective in secretion of these effectors, but that retain polar flagellum/motility, should be analyzed. Another NF-T3SS of *V. parahaemolyticus*, T3SS2, has been shown to be involved in delivering several effectors, such as VopA/P, VopC, VopV, VopT, and VopL[99,100]. A T3SS2-deficient *V. parahaemolyticus* was constructed by deleting the *vcrD2* gene, that has 25% of amino acid homology (Park et al. 2004; N. K. Lee and S. Park. unpublished result). This *ΔvcrD2* mutant demonstrated intact motility (H. J. Noh and S. Park.

unpublished result), suggesting that T3SS1 and T3SS2 of *V. parahaemolyticus* may function differentially with respect to flagellum biogenesis.

In addition to flagellar components, secretion of proteins that degrade or modify chitin decreased in the *ΔvcrD1* mutant[87]. Chitin supports *V. parahaemolyticus* growth and maintenance in a marine environment[101]. It also induces the expression of bacterial virulence factors, such as type IV pili[102]. It would be interesting to examine how these factors affect *V. parahaemolyticus* survival in marine environments.

V. CONCLUSION

V. parahaemolyticus is a marine bacterium that causes foodborne gastroenteritis. In this study, the roles of the two main virulence factors of *V. parahaemolyticus* were examined: thermostable direct hemolysin (Tdh) and type III secretion system 1 (T3SS1). At first, the expression patterns and cytotoxic role of Tdh were examined. Secondly, the role of VcrD1, a putative component of T3SS1, was evaluated in secretion and assembly of flagellar proteins of *V. parahaemolyticus*. The following conclusions were obtained through this study.

1. Transcriptional fusion assays indicated that expression of *tdhA* and *tdhS*, two genes encoding Tdh, is induced by iron chelator or crude bile. ToxR protein was found as a positive regulator mediating bile-induced expression of the *tdhA* gene. On the other hand, Fur and IscR do not play any role in iron-mediated of Tdh expression, suggesting the presence of another regulator for this process.

2. Treatment of human gastrointestinal cell line, HT-29, with rTdhA protein indicated that TdhA is capable of inducing cell death via apoptotic and necrotic pathways. However, rTdhA-induced cell death occurs more closely to necrosis.

3. Comparative proteomic analysis between the wild-type and *vcrD1* mutant (postulated to be TTSS1-defective) revealed that a majority of the down-secreted proteins in the *ΔvcrD1* mutant were associated with parts of the polar flagellum.

Subsequent study of bacterial flagella and motility indicated that the *ΔvcrD1* mutant does not have a polar flagellum or motility. Complementation of the wild-type *vcrD1* gene into the *ΔvcrD1* mutant restored bacterial motility. These results indicate that VcrD1, a component of TTSS1, is involved in the secretion of flagellar components in *V. parahaemolyticus.*

REFERENCES

1. Joseph S, Colwell R, Kaper J. *Vibrio parahaemolyticus* and related halophilic vibrios. Crit Rev Microbiol 1982;10(1):77–124.

2. Miwatani T, Takeda Y. *Vibrio parahaemolyticus'* epidemiology, ecology and biology. Saiko Tokyo Japan 1975;22–4.

3. Twedt RM. *Vibrio parahaemolyticus*. Foodborne Bacterial pathogens 1989;543–600.

4. Broberg CA, Calder TJ, Orth K. *Vibrio parahaemolyticus* cell biology and pathogenicity determinants. Microbes Infect 2011;13:992-1001.

5. Wagatsuma S. On a medium for hemolytic reaction. Media Circle 1968;13:159–62

6. Sakazaki R, Tamura K, Nakamura K, Kurata T, Gohda A, Kazuno Y. Studies on enterophathogenic activity of *Vibrio parahaemolyticus* using ligated gut loop model in rabbits. Jap J Med Sci Biol 1974;27:35–43.

7. Hueck CJ. Type III protein secretion systems in bacterial pathogens of animals and plants. Microbiol Mol Biol Rev 1998;62:379–433.

8. Park KS, Ono T, Rokuda M, Jang MH, Okada K, Iida T, et al. Functional characterization of two type III secretion systems of *Vibrio parahaemolyticus*.

Infect Immun 2004;72:6659 – 65.

9. Okuda J, Ishibashi M, Abbott I, Janda J, Nishibuchi M. Analysis of the thermostable direct hemolysin (*tdh*) gene and the tdh-related hemolysin (*trh*) genes in the urease-positive strains of *Vibrio parahaemolyticus* isolated on the West Coast of the United States. J Clin Microbol 1997;35:1965–71.

10. Nakaguchi Y, Okuda J, Iida T, Nishibuchi M. The urease gene cluster of *Vibrio parahaemolyhticus* does not influence the expression of the thermostable direct hemolysin gene or the TDH-related hemolysin gene. Microbiol Immunol 2003;47:233–9.

11. Nishibuchi M, Kaper J. Duplication and variation of the thermostable direct haemolytisin (*tdh*) gene in *Vibrio parahaemoltyicus*. Molec Microbiol 1990;4:87–99.

12. Miyamoto Y, Obara Y, Nikkawa T, Yamai S, Kato T, Yamada Y, et al. Simplified purification and biophysicochemical characteristics of Kanagawa phenomenon-associated hemolysin of *Vibrio parahaemolyticus*. Inf Immun 1980;28:567–76.

13. Douet J, Castroviejo M, Dodin A, Bebear C. Purification and characterization of Kanagawa haemolysin from *Vibrio parahaemolyticus*. Res Microbiol 1992;143:569–77.

14. Sakurai J, Matsuzaki A, Miwatani T. Purification and characterization of thermostable direct hemolysin of *Vibrio parahaemolyticus*. Infect Immun

1973;8:775–780.

15. Chun D, Chung J, Tak R. Some observations on Kanagawa type hemolysis of *Vibrio parahaemolyticus*. Tokyo Saikon Publ Co 1974;99–204.

16. Takahashi A, Yamamoto C, Kodama T, Yamashita K, Harada N, Nakano M, et al. Pore formation of thermostable direct hemolysin secreted from *Vibrio parahaemolyticus* in lipid bilayers. Int J Toxicol 2006;25(5):409-18.

17. Honda T, Iida T. The pathogenicity of *Vibrio parahaemolyticus* and the role of the thermostable direct heamolysin and related heamolysins. Rev Med Microbiol 1993;4:106–13.

18. Raimondi F, Kao JPY, Fiorentini C, Fabbri A, Donelli G, Gasparini N, et al. Enterotoxicity and cytotoxicity of *Vibrio parahaemolyticus* thermostable direct hemolysin in in vitro systems. Infect Immun 2000;68:3180–85.

19. Tang GQ, Iida T, Inoue H, Yutsudo M, Yamamoto K, Honda T. A mutant cell line resistant to *Vibrio parahaemolyticus* thermostable direct hemolysin(TDH): its potential in identification of putative receptor for TDH. Biochim Biophys Acta 1997;1360:277–82.

20. Yanagihara I, Nakahira K, Yamane T, Kaieda S, Mayanagi K, Hamada D, et al. Structure and functional characterization of *Vibrio parahaemolyticus* thermostable direct hemolysin. J Biol Chem 2010;285(21):16267-74.

21. Oliver JD. Formation of viable but nonculturable cells. American Society for Microbiology 1993;239–72.

22. Cotter PA, Dirita VJ. Bacterial virulence regulation: an evolutionary perspective. Annu Rev Microbiol 2000;54:519–65.

23. Matson JS, Withey JH, DiRita VJ. Regulatory networks controlling *Vibrio cholerae* virulence gene expression. Infect Immun 2007;75:5542–9.

24. Jordi T, Elisa C, Joaquim R. Oxidative stress in bacteria and protein damage by reactive oxygen species. Internatl Microbiol 2000; 3:3–8.

25. Andrews SC, Robinson AK. Rodriguez-Quinones F: Bacterial iron homeostasis. FEMS Microbiol Rev 2003;27:215–37.

26. Masse E, Arguin M. Ironing out the problem: new mechanisms of iron homeostasis. Trends Biochem Sci 2005;30:462–68.

27. Calderwood SB, Mekalanos JJ. Iron regulation of Shiga-like toxin expression in *Escherichia coli* is mediated by the fur locus. J Bacteriol 1987;169:4759–64.

28. Stoebner JA, Payne SM. Iron-regulated hemolysin production and utilization of heme and hemoglobin by *Vibrio cholerae.* Infect Immun 1988;56:2891–95.

29. Tao X, Schiering N, Zeng HY, Ringe D, Murphy JR. Iron, DtxR, and the regulation of diphtheria toxin expression. Mol Microbiol 1994;14:191–7.

30. De Lorenzo V, Giovannini F, Herrero M, Neilands JB. Metal ion regulation of gene expression, Fur repressor-operator interaction at the promoter region of the aerobactin system of pColV-K30. J Mol Biol 1988;203:875–84.

31. Escolar L, Perez-Martin J, de Lorenzo V. Opening the iron box: transcriptional metalloregulation by the Fur protein. J Bacteriol 1999;181:6223–9.

32. Miyamoto K, Kosakai K, Ikebayashi S, Tsuchiya T, Yamamoto S, Tsujibo H. Proteomic analysis of *Vibrio vulnificus* M2799 grown under iron-repleted and iron-depleted conditions. Microb Pathog 2009;46:171–7.

33. Fontecave M. Iron-sulfur clusters: ever-expanding roles. Nat Chem Biol 2006;2:171–4.

34. Py B, Barras F. Building Fe-S proteins: bacterial strategies. Nat Rev Microbiol 2010;8:436–46.

35. Schwartz CJ, Giel JL, Patschkowski T, Luther C, Ruzicka FJ, Beinert H, et al. IscR, an Fe-S cluster-containing transcription factor, represses expression of *Escherichia coli* genes encoding Fe-S cluster assembly proteins. Proc Natl Acad Sci USA 2001;98:14895–900.

36. Lim JG, Choi SH. IscR Is a Global Regulator Essential for Pathogenesis of *Vibrio vulnificus* and Induced by Host Cells. Infect Immun 2014;82(2):569-78.

37. Noh DO, Gilliland SE. Influence of bile on cellular integrity and b-galactosidase

activity of *Lactobacillus acidophilus*. J Dairy Sci 1993;76:1253–59.

38. Miller VL, Mekalanos JJ. Synthesis of cholera toxin is positively regulated at the transcriptional level by toxR. Proc Natl Acad Sci USA 1984;81:3471–75.

39. DiRita VJ, Parsot C, Jander G, Mekalanos JJ. Regulatory cascade controls virulence in *Vibrio cholerae*. Proc Natl Acad Sci USA 1991;88:5403–7.

40. Deborah T, John J. Bile acids induce cholera toxin expression in *Vibrio cholerae* in a ToxT-independent manner. PNAS 2005;102(8):3028-33.

41. Provenzano D, Klose KE. Altered expression of the ToxR-regulated porins OmpU and OmpT diminishes *Vibrio cholerae* bile resistance, virulence factor expression, and intestinal colonization. Proc Natl Acad Sci USA 2000;97:10220–4

42. Bina J, Zhu J, Dziejman M, Faruque S, Calderwood S, Mekalanos J. ToxR regulon of *Vibrio cholerae* and its expression in vibrios shed by cholera patients. Proc Natl Acad Sci USA 2003;100:2801–6.

43. LEE JW. The effects of *Vibrio parahaemolytiucs* thermostable direct hemolysin on the host cell death. Yonsei Univ.;2011.

44. Jeong HS, Jeong KC, Choi HK, Park KJ, Lee KH, Rhee JH, et al. Differential expression of *Vibrio vulnificus* elastase gene in a growth phasedependent manner by two different types of promoters. J Biol Chem 2001;27:13875–80.

45. Milton DL, O'Toole R, Horstedt P, Wolf-Watz H. Flagellin A is essential for the virulence of *Vibrio anguillarum*. J Bacteriol 1996;178:1310–9.

46. Lee JH, Rho JB, Park KJ, Kim CB, Han YS, Choi SH, et al. Role of flagellum and motility in pathogenesis of *Vibrio vulnificus*. Infect Immun 2004;72:4905-10.

47. Keen NT, Tamaki S, Kobayashi D, Trollinger D. Improved broad-host-range plasmids for DNA cloning in Gram-negative bacteria. Gene 1998;70:191-7.

48. Simon R, Priefer U, Pulher A. A broad host range mobilisation system for in vivo genetic engineering: transposon mutagenesis in gram-negative bacteria. Bio/Technology 1983;1:784–91.

49. Escolar L, Perez-Martin J, de Lorenzo V. Opening the iron box: transcriptional metalloregulation by the Fur protein. J Bacteriol 1999;181:6223–9.

50. Hofmann AF. Bile Acids: The good, the bad, and the ugly. Gastrointestinal and Liver Disease 1999;14:937–48.

51. Mekalanos JJ. Duplication and amplification of toxin genes in *Vibrio cholerae*. Cell 1983;35:253–63.

52. Park KS, Ono T, Rokuda M, Jang MH, Iida T, Honda T. Cytotoxicity and enterotoxicity of the thermostable direct hemolysin-deletion mutants of *Vibrio parahaemolyticus*. Microbiol Immunol 2004;48:313–8.

53. Vandenabeele P, Galluzzi L, Berghe TV, Kroemer G. Molecular mechanisms of necroptosis: an ordered cellular explosion. Nature 2010;11(10):700-14.

54. Miyamoto Y, KatoT, Obara Y, Akiyama S, Takizawa K, Yamai S. In vitro hemolytic characteristic of *Vibrio parahaemolyticus*: its close correlation with human pathogenicity. J Bacteriol 1969;100:1147–9.

55. Sakazaki R, Tamura K, Kato T, Obara Y, Yamai S, Hobo K. Studies on the enteropathogenic, facultatively halophilic bacterium, *Vibrio parahaemolyticus.* II. Serological characteristics. Jpn J Med Sci Biol 1968;21:313–24.

56. Honda T, Chearskul S, Takeda Y, Miwatani T. Immunological methods for detection of Kanagawa phenomenon of *Vibrio parahaemolyticus*. J Clin Microbiol 1980;11:600–3.

57. Ljungh A, Wadstro¨m T. Toxins of *Vibrio parahaemolyticus* and Aeromonas hydrophila. J Toxicol Toxin Rev 1982;1:257–307.

58. Takeda Y. Thermostable direct hemolysin of *Vibrio parahaemolyticus.* Pharmacol Ther 1983;19:123–46.

59. Park KS, Ono T, Rokuda M, Jang MH, Iida T, Honda T. Cytotoxicity and enterotoxicity of the thermostable direct hemolysin-deletion mutants of *Vibrio parahaemolyticus.* Microbiol Immunol 2004;48:313–8.

60. Nishibuchi M, Honda T, Miwatani T, Kaper JB. Diversity and possible mobility

of the tdh gene of *Vibrio parahaemolyticus* and related hemolysin genes. KTK Scientific Publishers Tokyo 1990;7:173–9.

61. Lin Z, Kumagai K, Baba K, Mekalanos JJ, Nishibuchi M. *Vibrio parahaemolyticus* has a homolog of the *Vibrio cholerae toxRS* operon that mediates environmentally induced regulation of the thermostable direct hemolysin gene. J Bacteriol 1993;175:3844–55.

62. Oliver JD, Hite F, McDougald D, Andon NL, Simpson LM. Entry into, and resuscitation from, the viable but nonculturable state by *Vibrio vulnificus* in an estuarine environment. Appl Environ Microbiol 1995;61:2624–30.

63. Park KJ, Kang MJ, Kim SH, Lee HJ, Lim JK, Choi SH, et al. Isolation and Characterization of rpoS from a Pathogenic Bacterium, *Vibrio vulnificus*: Role of sigma S in Survival of Exponential-Phase Cells under Oxidative Stress. J Bacteriol 2004;186(11):3304-12.

64. Kim IH, Wen Y, Son JS, Lee KH, Kim KS. The Fur-Iron Complex Modulates Expression of the Quorum-Sensing Master Regulator, SmcR, To Control Expression of Virulence Factors in *Vibrio vulnificus*. Infect Immun 2013;81(8):2888-98.

65. Wu Y, Outten FW. IscR controls iron-dependent biofilm formation in *Escherichia coli* by regulating type I fimbria expression. J Bacteriol 2009;191:1248–57.

66. Jovanovic G, Weiner L, Model P. Identification, nucleotide sequence, and characterization of PspF, the transcriptional activator of the *Escherichia coli* stressinduced psp operon. J Bacteriol 1996;178:1936–45.

67. Darwin AJ, Miller VL. The psp locus of *Yersinia enterocolitica* is required for virulence and for growth in vitro when the Ysc type III secretion system is produced. Mol Microbiol 2001;39:429–44.

68. Beloin C, Valle J, Latour-Lambert P, Faure P, Kzreminski M, Balestrino D, et al. Global impact of mature biofilm lifestyle on *Escherichia coli* K-12 gene expression. Mol Microbiol 2004;51:659–74.

69. Goldberg MB, Boyko SA, Calderwood SB. Positive transcriptional regulation of an iron-regulated virulence gene in *Vibrio cholerae*. Proc Natl Acad Sci USA 1991;88:1125-9.

70. Rogers SD, Bhave MR, Mercer JF, Camakaris J, Lee BT. Cloning and characterization of cutE, a gene involved in copper transport in *Escherichia coli.* J Bacteriol 1991;173(21):6742-8.

71. Mekalanos JJ. Duplication and amplification of toxin genes in *Vibrio cholerae.* Cell 1983;35:253–63.

72. Arends MJ, Wyllie AH. Apoptosis: mechanisms and roles in pathology. Int Rev Exp Pathol 1991;32:223-54.

73. Naim R, Yanagihara I, Iida T, Honda T. *Vibrio parahaemolyticus* thermostable direct hemolysin can induce an apoptotic cell death in Rat-1 cells from inside and ouside of the cells. FEMS Microbiology Letters 2001;195:237–44.

74. Honda T, Ni Y, Miwatani T, Adachi T, Kim J. The thermostable direct hemolysin of *Vibrio parahaemolyticus* is a pore forming toxin. Can J Microbiol 1992;38:1175–80.

75. Daniels NA, MacKinnon L, Bishop R, Altekruse S, Ray B, Hammond RM, et al. *Vibrio parahaemolyticus* infections in the United States. J Infect Dis 2000;181:1661-6.

76. Nair GB, Ramamurthy T, Bhattacharya SK, Dutta B, Takeda Y, Sack DA.Global dissemination of *Vibrio parahaemolyticus* serotype O3:K6 and its serovariants. Clin Microbiol Rev 2007;20:39-48.

77. Makino K, Oshima K, Kurokawa K, Yokoyama K, Uda T, Tagomori K, et al. Genome sequence of *Vibrio parahaemolyticus*: a pathogenic mechanism distinct from that of *V. cholerae*. Lancet 2003;361:743-9.

78. Yang YJ, Lee NK, Lee NY, Lee JW, Park SJ. Cell death mediated by *Vibrio parahaemolyticus* type III secretion system 1 is dependent on ERK1/2 MAPK, but independent of caspases. J Microbiol Biotechnol 2011;21:903-13.

79. Macnab RM. Type III flagellar protein export and flagellar assembly. Biochim Biophy Acta 2004;1694:207-7.

80. Abby SS, Rocha EP. The non-flagellar type III secretion system evolved from the bacterial flagellum and diversified into host-cell adapted systems. PLOS Genet 8:e1002983.

81. McCarter LL. The multiple identities of *Vibrio parahaemolyticus*. J Mol Microbiol Biotechnol 1999;1:51-7.

82. Duan Q, Zhou M, Zhu L, Zhu G. Flagella and bacterial pathogenicity. J Basic Microbiol 2013;53(1):1-8.

83. Belas R, Simon M, Silverman M. Regulation of lateral flagella gene transcription in *Vibrio parahaemolyticus*. J Bacteriol1986;167(1):210-8.

84. Kim Y, McCarter LL. Analysis of the polar flagellar gene system of *Vibrio parahaemolyticus*. J Bacteriol 2000;182:3693-704.

85. McCarter LL. Polar flagellar motility of the Vibrionaceae. Microbiol Mol Biol Rev 2001;65:445-62.

86. Manoil C, Beckwith J. A genetic approach to analyzing membrane protein topology Science 1986;233:1403-8.

87. Lee NK. Functional identification of type III secretion system 1 of *Vibrio parahaemolyticus*. Yonsei Univ.;2009.

88. Jorges EG. Energizing type III secretion machines: what is the fuel? Nat Struct Mol Biol 2008;15:127-8.

89. Lee JH, Rho JB, Park KJ, Kim CB, Han YS, Choi SH, et al. Role of flagellum and motility in pathogenesis of *Vibrio vulnificus*. Infect Immun 2004;72:4905-10.

90. Kutsukake K, Iino T. Role of the FliA-FlgM regulatory system on the transcriptional control of the flagellar regulon and flagellar formation in *Salmonella typhimurium.* J Bacteriol 1994;176:3598-605.

91. Buttner D. Protein export according to schedule: architecture, assembly, and regulation of type III secretion systems for plant- and animal-pathogenic bacteria. Microbiol Mol Biol Rev 2012;76:262-310.

92. Kim Y, McCarter LL. Cross-regulation in *Vibrio parahaemolyticus*: compensatory activation of polar flagellar genes by the lateral flagellar regulator LafK. J Bacteriol 2004;186:4014-8.

93. Aldridge P, Hughes KT. Regulation of flagellar assembly. Curr Opin Microbiol 2002;5:160-5.

94. Ohnishi K, Kutsukake K, Suzuki H, Lino T. A novel transcriptional regulation mechanism in the flagellar regulon of *Salmonella typhimurium*: an antisigma factor inhibits the activity of the flagellum-specific sigma factor, sigma F. Mol Microbiol 1992;6:3149-57.

95. Chilcott GS, Hughes KT. Coupling of flagellar gene expression to flagellar assembly in Salmonella enterica serovar *Typhimurium* and *Escherichia coli.*

Microbiol Mol Biol Rev 2000;64:694-708.

96. Burdette DL, Seemann J, Orth K. Vibrio VopQ induces PI3-kinase-independent autophagy and antagonizes phagocytosis. Mol Micriobiol 2009;73:639-49.

97. Yarbrough ML, Li Y, Kinch LN, Grishin NV, Ball HL, Orth K. AMPylation of Rho GTPases by Vibrio VopS disrupts effector binding and downstream signaling. Science 2009;323:269-72.

98. Matsuda S, Okada N, Kodama T, Honda T, Iida T. A cytotoxic type III secretion effector of *Vibrio parahaemolyticus* targets vacuolar H(+)-ATPase subunit C and ruptures host cell lysosomes. PLOS Pathog 2014;8:e1002803.

99. Zhang L, Orth K. Virulence determinants for *Vibrio parahaemolyticus* infection. Curr Opin Microbiol 2013;16:70-7.

100. Ham H, Orth K. The role of type III secretion system 2 in *Vibrio parahaemolyticus* pathogenicity. J Microbiol 2012;50:719-25.

101. Pace J, Chai TJ. Comparison of *Vibrio parahaemolyticus* grown in estuarine water and rich medium. Appl Environ Microbiol 1989;55:1877-87.

102. Frischkorn KR, Stojanovski A, Paranjpye R. *Vibrio parahaemolyticus* type IV pili mediate interactions with diatom-derived chitin and point to an unexplored mechanism of environmental persistence. Appl Environ Microbiol 2013;15:1416-27.

ABSTRACT (KOREAN)

장염비브리오균 병원성 인자인 Tdh와 VcrD1의 기능 분석

<지도교수 박 순 정>

연세대학교 대학원 의과학과

노 현 진

장염비브리오균은 그람 음성 세균으로서 전세계 바다에 서식하고 있으며 음식물을 통해 사람에게 감염되어 장염을 유발한다. 장염비브리오균이 가지고 있는 주요한 병원성 인자 중 하나로 thermostable direct hemolysin (Tdh)이 있으며 이것은 병원성 장염비브리오균이 가지는 Kanagawa 현상의 원인 인자이다. Chapter I에서는 다양한 배양 조건에서 Tdh 유전자 발현의 변화를 살펴보았다. 유전체 염기분석을 통하여 야생종 장염비브리오균이 두 개의 *tdh* 유전자 *tdhA*와 *tdhS* 를 가지고 있는 것이 밝혀졌다. *tdh*의 promoter와 luciferase 유전자의 fusion을 이용한 promoter 활성도를 측정한 결과, *tdhA*의 유전자의 발현은 *tdhS*보다 항상 높은 수준으로 나타났다. 또한, *tdh* 유전자의 발현은 iron chelator와 bile에 의하여 증가하였다. Bile의 존재 하에 *tdh*의 발현을 매개하는

전사 인자를 찾기 위하여 ligand fishing 실험을 수행하였다. 한편, 장염비브리오균의 *toxR* 돌연변이주의 western blot과 fusion assay를 통하여 bile에 의해 유도되는 *tdhA*의 전사 조절은 ToxR이 관여하고 있다는 것을 알아내었다. ToxR 단백질이 *tdhA* promoter 부분에 직접적으로 결합하는 것은 gel-shift assay로 확인하였다. 이외에도 숙주 세포에 대한 TdhA 단백질의 세포 독성능을 알아보았다. TdhA 단백질을 인간의 장 세포에 처리하였을 때 형태학적으로 상당한 변형이 일어나는 것을 전자현미경을 통하여 관찰하였다. Annexin V와 PI 염색을 통해 TdhA 세포 독성능은 apoptosis와 necrosis가 모두 관여하고 있는 것을 알 수 있었다. Necrostatin-1에 의하여 TdhA의 세포 독성능이 감소하는 것은 TdhA에 의해 유도되는 세포 사멸 과정에 RIP-1 mediated necroptosis가 포함되어 있음을 나타낸다. 이러한 결과들로 미루어보아 *tdh*의 유전자 발현은 철 이온의 양, 또는 bile과 같은 특정한 환경 인자에 의하여 조절되고, 만들어진 Tdh 단백질은 necrosis을 포함한 다양한 방식으로 숙주 세포 사멸을 유도한다고 할 수 있다.

Chapter II에서는 장염비브리오의 type III secretion system (T3SS) 의 구성 성분 중 하나인 *vcrD1*에 대하여 공부하였다. 장염비브리오균의 야생종과 VcrD1의 돌연변이주의 총 분비단백질을 비교 분석한 결과 돌연변이주는 야생종에 비하여 19개의 단백질의 분비에 결함이 생긴 것이 밝

혀졌다. 그 단백질 중 일부는 편모의 구성 성분을 포함하고 있다. 야생종과 돌연변이주의 총 분비단백질을 FlaA, FlgL, FlgE 그리고 FlaM 단백질에 각각 특이성이 있는 항체를 이용하여 western blot 분석 방법으로 조사하였다. 그 결과, 적어도 이 4가지의 편모 구성 성분들의 분비가 돌연변이주에서 영향을 받았다는 것을 확인 할 수 있었다. *vcrD1* 돌연변이주는 운동성이 없어졌으며, 전자 현미경 관찰에서도 편모가 없어진 형태를 보였다. 이 돌연변이주에 야생종 *vcrD1* 유전자를 플라스미드에 삽입시켜 회복시킨 균주는 운동성이 다시 나타나는 것을 확인하였다. 세포 분획 방법으로 세균을 세포질, 주변세포질, 세포막으로 나누어 관찰한 결과 FlaA와 FlgM은 야생종에 비하여 *vcrD1*에서 모두 감소하였다. 이것은 *vcrD1*의 돌연변이주에서 편모의 구성 성분들의 유전자 발현과 단백질 분비가 모두 영향을 받았다는 것을 나타낸다. 편모 구성 성분 중에서 대표적인 7개의 유전자를 가지고 수행한 RT-PCR 결과 초기에 발현되는 편모 유전자는 *vcrD1* 돌연변이주에서 영향이 없었지만, 중간과 후기에 발현되는 유전자들은 돌연변이주에서 RNA 수준이 감소하였다. 따라서 장염비브리오의 VcrD1은 편모 구성 성분의 유전자 발현과 단백질 분비를 조절함으로써 편모의 형성과정에 중요한 역할을 한다고 여겨진다.

핵심되는 말: *vibrio parahaemolyticus*, thermostable direct hemolysin, *vcrD1*